A Two-Stage Formation Flying Strategy for UAVs

Chong Xiang

A Thesis

in

The Department

of

Electrical and Computer Engineering

Presented in Partial Fulfillment of the Requirements

for the Degree of Master of Applied Science at

Concordia University

Montréal, Québec, Canada

2006

Your file Votre référence
ISBN: 978-0-494-28932-7
Our file Notre référence
ISBN: 978-0-494-28932-7

ABSTRACT

A Two-Stage Formation Flying Strategy for UAVs

Chong Xiang

This thesis is concerned with formation flying of unmanned air vehicle (UAV) with minimum time mission requirement. It is assumed that a known finite set of different configurations exists, which characterizes the mission. This means that the desired configuration at each point in time belongs to this set. A reconfiguration strategy is then introduced which is carried out in two phases. The first phase starts upon the completion of the latest reconfiguration task. In this phase, each UAV moves to a pre-determined location which is obtained to be as close as possible to all potential next destinations given by the known set. All UAVs stay in this location during the idle time, i.e., while no new mission command is issued. The second phase begins once a new command is issued to reconfigure the formation. In this phase, all UAVs will move to the location specified by the new command. This two-stage strategy minimizes the reconfiguration time, which is quite desirable in many real-world applications. Simulation results demonstrate that the proposed strategy results in a significant reduction in the reconfiguration time.

"Yes, we have to divide up our time like that, between our politics and our equations. But to me our equations are far more important, for politics are only a matter of present concern. A mathematical equation stands forever.." —Albert Einstein

I dedicate this work to my great family, father (XuHui), mother (JiXiu), brother (Sheng), and sister (JiaJia), for their love, encourage, and warm comfort throughout my life. Without them, I could not finish my job. Although they are not here, Montreal, Canada, I always can feel them around me and support me.

ACKNOWLEDGEMENTS

I would like to thank my supervisor Dr. Amir G Aghdam for his strong support on this work by his knowledge, encourage, and patience, and so on.

I would appreciate the passionate encourage of my best friend, Haijiang He and his wife, Wuran Lv, Lei Feng and his wife Huijun Zhang, Yu Yang and Feifei Cao and my classmate Tousi Mani, Idin Karuei, and other kind and professional people of the group throughout these years.

I would also appreciate the help from many friends I can not name them here.

I truly appreciate those people who have enriched me as a man and master student. I think I can not use my poor language to describe my thankfulness to them. I sincerely thank them because I would not be who I am without them.

TABLE OF CONTENTS

LIST OF FIGURES

Chapter 1

Introduction

There has been a considerable amount of interest towards cooperative control of a group of vehicles in the past several years [1], [2]. In particular, precision control of unmanned air vehicles (UAV) flying in formation has been investigated intensively in the literature in recent years [3], [4]. Due to increasing need for missions involving UAVs, a great deal of research is currently being carried out both independently and collaboratively by several countries, including Canada. For instance, some details of projects of this type in operation enduring freedom (OEF) and operation Iraqi freedom (OIF) are reported in [5], [6] and [7].

Since 1950s, UAVs have been used in several missions of the U.S.Air Force. Prior to that, in 1920s, very simple forms of UAVs with open loop control configuration were developed for military aims [5].

More recently, UAVs have been deployed for several types of missions in different environments. For example, in OIF, UAVs were used in the time sensitive missions. According to [6], a UAV called Global Hawk, was used in 16 missions within 45 days to locate important targets for the missiles. The information collected by the UAV was used in fifty surface-to-air missile (SAM) launchers and more than three hundred tanks. Nowadays, UAVs can be deployed in twenty-four-hour missions. Some of them, for example, RQ-4A global hawk, can reach the maximum speed of 350kt (180 m/s). UAVs are also used to collect data by taking pictures in dangerous environments such as reconnaissance missions in the battle field. They can be utilized for long distance and long time flying missions. The future UAV missions are anticipated to require very high precision with a greater confidence of mission accomplishment.

Some of the future projects involving military applications for UAVs are described in [5], where four essential components are introduced as the building blocks for UAVs. These main components consist of processor, communication, platform, and payload. The main focus of the researchers in this area is to improve reliability, robustness, precision and flexibility, and to reduce cost. These are the main design specifications, in both military and civilian missions.

Several civilian UAV missions, such as forest fire mapping, detection and fight, require UAVs to fly cooperatively [4]. In forest fire detection, UAVs are employed to fly over the fire field to detect the range of fired forest and transfer corresponding data to base station as soon as possible. Several UAVs have been used in forest fire fighting since 1990s

in U.S.A and China.

Some of the recent UAV missions such as the ones involving taking pictures from a battle field require cooperative work. For a better reliability, equipments are sometimes split into different parts and are put into different UAVs. If one of the UAVs and the equipment corresponding to that fails, others can still accomplish the job. For this purpose, UAVs must fly in special positions, in order for the entire group to fly in a desired formation. Formation control is a very important and interesting field, which can be categorized as a cooperative control system. Formation flying is used in both military and civilian applications, in order to achieve precision in accomplishing the mission.

Five categories of formation flying architectures are introduced in [1] and [2]: multiple-input multiple-output (MIMO), leader/follower (L/F), virtual structure (VS), cyclic, and behavioral. Formation problems appear also in robotics and satellite applications. In some communication problems such as airborne communication node (ACN) applications, UAVs are exploited to represent nodes of a communication system in order to improve reliability and performance of the overall system. This is accomplished by placing several UAVs in certain locations in the space.

Formation flying can be regarded as a multi-input multi-output system. Thus, all modern control tools such as LQR design can be used in a MIMO framework, in order to find a high-performance controller. This method is very effective when the number of the nodes in the formation configuration is relatively small. For large formation architectures

where several hundred nodes of the formation are required to be controlled, the computational complexity limits the effectiveness of the MIMO approach significantly. In such cases, decentralized control theory can be a desirable alternative to reduce computational effort by implementing local controllers with minimum communication requirement between them [8], [9]. More recently, nonlinear control theory has been utilized in MIMO formation flying control [10].

In the MIMO formation architecture, the existing techniques are employed to obtain the proper controller for the formation flying. These techniques are, in general, suitable for the problems with relatively small number of nodes. For formation applications with a huge number of nodes, however, the control design problem can be quite cumbersome.

Leader/follower (L/F) is a very popular architecture in formation flying. In this approach, one of the vehicles acts as the leader, sends the required command to other followers, and dose not receive any feedback from them. This is conceptually similar to the master/slave structure. Some important features of the L/F architecture are introduced in [2]. Mesh stability and exponential mesh stability were discussed for this type of architecture in [11], and the results were used in nonlinear control framework to verify the stability of the L/F formation control system.

In virtual structure (VS) formation flying control, all UAVs are regarded as one rigid body. The main difference between the L/F and VS approaches is that in the latter architecture the leader needs to obtain the required information from other UAVs, while in

the former one the leader sends the commands to the followers regardless of their current situation. As a results, the control configuration in the L/F approach is open-loop, which can cause significant problems such as error propagation, poor robustness, etc., in general. Iterated VS (IVS) and guidance VS (GVS) are two types of virtual structures which are employed in different missions [12], [13] .

Cyclic approach is similar to the L/F from the control standpoint in terms of the communication between the UAVs. The main difference in this case is that the cyclic architecture is not hierarchical. It is hard to obtain stability results for cyclic architecture because it directly depends on the interconnection structure. In other words, the stability of each vehicle depends on other connected vehicles. A methodology is proposed in [14] to control each vehicle with respect to the center-of-mass of a set of its neighbors.

Behavioral architecture is usually used along with other architectures such as L/F and cyclic. It mainly focuses on maintaining formation and avoiding collision for each vehicle. For example, a behavioral algorithm was introduced in [15], which considers the velocity vector as the behavior factor for vehicles. The disadvantages of behavioral architecture are as follows: First, it is very difficult to obtain the mathematical model for the system from completed behaviors. Second, it is not easy to verify the desired behaviors along with other algorithms. As a matter of fact, simulation is the only verification tool in this case [2].

The above mentioned formation architectures have been thoroughly investigated

in the literature in the past several years. For instance, identification and control synthesis were studied in [16]. Furthermore, a method was proposed in [17] to direct the UAVs to their desired positions with minimum fuel cost. A robust optimal decentralized formation control technique for L/F was also introduced in [8].

The minimum time control strategy in formation flying of UAVs was investigated in [4], where it was desired that UAVs switch from one formation to another as quickly as possible. It is to be noted that a faster switching between formations means a smaller mission time. Formulation of optimal fuel-cost problem for UAVs switching as well as the corresponding analytical results are presented in [18]. Since in most applications it is desired to accomplish the mission in a short period of time with small fuel consumption, a mixed time-fuel optimization in formation switching and reconfiguration is of a great interest in practice. The significance of formation switching or reconfiguration in unmanned aerial combat vehicles (UACV) is also discussed in [3].

An algorithm for time-critical missions of several UAVs in formation flying with collision avoidance was introduced in [19]. Furthermore, a direct solution for the fuel-optimal problem with reactive collision avoidance for spacecraft formation flying was proposed in [20]. Various methods and ideas provided in the literature to solve relevant problems in formation flying for UAVs in recent years [21], [22], [23].

Different control strategies have been investigated in the literature to meet a wide

variety of design objectives. The problem is first formulated in an optimal control framework, and then solved to find a control strategy which minimizes a given cost function. However, while there is a closed-form solution for minimum energy problem (i.e., quadratic cost function), only numerical methods may be feasible for solving the problem in general case. This may require undesirably high computation capability. Furthermore, due to the communication constraints in most flight formation problems, the preferred control structure for this type of applications is decentralized [9], [24]. In other words, it is desired to obtain a set of local controllers for the set of UAVs to operate independently from each other. All controllers are involved, however, in the overall operation of the system. It is known that the optimal control design problem is even more cumbersome for decentralized systems. As a matter of fact, unlike the centralized case, the closed-form solution for the optimal decentralized control strategy with respect to a quadratic performance index may be very complex and prone to robustness problems [8].

In this thesis, a new algorithm is introduced to minimize the reconfiguration time in formations flying of UAVs. The proposed algorithm reduces the mission time for all UAVs and all possible reconfigurations. In other words, the algorithm provides minimum average time over all formations and for all UAVs. First, it is assumed that each UAV can switch to the new position independently of all other UAVs (in terms of control). This means that the UAVs will be regarded as non-coupled models when they switch formation (for the sake of simplicity). It is also assumed that the set of all possible locations (preferably with the probability corresponding to each location) is given. This implies that all

required computations will be carried out off-line. Another important assumption made is that there is a sufficiently long idle time between two consecutive formation reconfiguration. In other words, once a formation mission is accomplished, there will be a sufficiently long period of time for the UAVs to settle down before the next mission starts.

In order to simplify the problem, the algorithm will consider the position switching of the individual UAVs in the formation, one by one. Then, an optimal position will be obtained for each UAV with the property that it is the closest position to all possible locations (with the corresponding probabilities, if available) time-wise. The optimal formation corresponding to the idle-time position of all UAVs can then be obtained accordingly. This idle-time formation is the closest configuration to all possible formations, and hence can be used to save time in switching between different configurations.

For simplicity of analysis, it is also assumed that UAVs fly with a constant speed, so that one can relate the switching time for the *ith* UAV to its speed $|\vec{V}_i|$ and relative distance between its positions before and after switching $\vec{d}_i$, by the simple zero-acceleration equation $T_i = \frac{|\vec{d}_i|}{|\vec{V}_i|}$. Note that the reference frame will be leader frame throughout this thesis. It will also be shown that the proposed algorithm can help reduce the fuel consumption to some extent for different missions.

Chapter 2

Overview of Formation Flying of Unmanned Aerial Vehicles

Unmanned Aerial Vehicles (UAVs) are auto-piloted or remote-piloted aircrafts that can carry several kinds of payloads, such as cameras, sensors, and communication systems. Since 1950s (or even prior to that), they have been used in many missions. More recently, a group of UAVs have been used as a team to accomplish different mission with high precision. For example, a group of three UAVs flying as a triangle is a typical flight formation which has been used in different applications [3]. Formation flying of UAVs is becoming increasingly important for applications of different nature; e.g. civilian and military.

2.1 The Kinematic Model of UAVs

Operation of the UAV is characterized by a kinematic description which is based on the well-known Frenet-Serret equations of motion. The kinematic model of UAV is often introduced as a reduced order dynamic model in a two-dimensional frame [25], [26], [18], [27].

Consider Figure 2.1, where (x,y), ψ, V, and ω represent the inertial position, aircraft heading angle, velocity, and the turning rate of the UAV, respectively. Furthermore, let u, ω_{max} and Td denote the rate command, the maximum allowable turning rate, and the actuator delay, respectively. Then, the resulting kinematic equations of motion are:

$$\begin{aligned} \dot{x}(t) &= V\cos(\psi(t)) \\ \dot{y}(t) &= V\sin(\psi(t)) \\ \dot{\psi}(t) &= \omega(t) \\ \omega(t) &= u(t-Td) \end{aligned} \tag{2.1}$$

The input constraints are $V_{min} \leq V \leq V_{max}$, $|u| \leq \omega_{max}$, and $\omega_{min} \leq \omega \leq \omega_{max}$. If the velocity V is constant, then the equation (2.1) will be the same as the one given in [26]. If it is not constant, then one can follow a method similar to the ones in [25] and [28] to find more detailed characteristics.

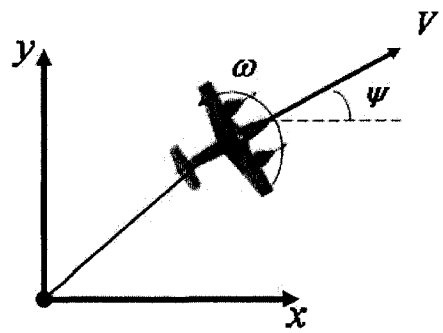

Figure 2.1: The low-level autopilot with a 2-D model

2.2 Overview of Formation Architectures

Formation flying is defined as a set of more than one vehicle (e.g., multiple UAVs, space-craft, etc.), whose states are coupled through a common control law [1], [2]. Five main formation flying control (FFC) architectures are introduced in [1], [2] as leader/follower, virtual structure, behavioral, multiple-input multiple-output, and cyclic.

2.2.1 Leader/Follower

The leader/follower (L/F) architecture is one of the primary architectures of FFC, and is sometimes referred to as master/slave [29] and chief/deputy [30]. The main characteristic of L/F architecture is that it considers multiple vehicles as one hierarchical system, where each subsystem has its own local controller. Utilization of a decentralized control configuration instead of a centralized one can reduce the formation control design for a complex system

to the design of a set of simple individual controllers. It is to be noted that one of the main design objectives for this type of control problems is good tracking capabilities.

Some important definitions will now be introduced briefly. Consider a directed graph consisting of a set of edges $\mathcal{E}$, a set of vertices V, and an optional set of weights W. The pair (i, j) represents an edge from i to j, for any $i,j \in$ V. This directed graph is sometimes referred to as dependency digraph [2]. The vertices (nodes) of the dependency graph are used to indicate vehicles in formation flying. If, for example, the control action of vehicle j is dependent on the state of vehicle i, this will be represented by a directed edge (i, j) in the digraph. The following three conditions can produce the directed edge (i, j) in the dependency digraph.

1. A relative state function of vehicle i and j is being tracked by vehicle j;
2. The reference trajectory of vehicle j is a function of the state of vehicle i;
3. The controller of vehicle j is using a feedback signal from vehicle i.

A L/F FFC algorithm, in fact, considers the interconnected individual controllers of a group of vehicles in an acyclic control dependency directed graph. From a graph theoretic viewpoint, an edge (i,j) indicates that vehicle j is a follower and vehicle i is a leader. It is to be noted that a vehicle can, in general, have more than one leader [31]. Sometimes, however, the term single leader L/F is used to emphasize that each follower has only one leader [1], [2], [10], [32].

Mesh stability (exponential mesh stability) was first introduced for linear systems in [11] and the results were later extended to nonlinear systems. More specifically, the sufficient conditions for the stability of L/F FFC in mesh stability sense were applied to nonlinear systems. It was also shown in [2] that if a L/F formation system is asymptotically Lyapunov stable, it is asymptotically mesh stable as well. The concept of mesh stability in formation flying was developed analogously to the concept of string stability in automated highway system (AHS) and large platoon of vehicles [33]. Two sufficient conditions are given for the mesh stability [11]. The first condition is the exponential stability of the dynamics of the individual subsystems. The second condition is that the interconnections between subsystems are globally Lipschitz in their arguments.

In the case of single leader L/F systems, two different types of formation are being investigated in the literature. Some researchers consider multiple followers with the same leader; while some other are mainly focused on the string formation such that each vehicle follows the one ahead of it.

On the other hand, the area of deep space (DS) and planetary orbital environment (POE) has been the main focus of several long-term projects since 1980s, and has attracted a lot of researchers in the area of spacecraft formation in the past decade. A great deal of the works in this field have been concerned with the time optimal and fuel optimal control problems. One of the most common approaches used by the researchers to tackle this problem has been the control design based on Hill-Clohessy-Wiltshire (HCW) equations. For instance, a discrete-time controller was developed for pulse-based actuators,

and a LQG controller was designed based on the measurements by the Global Positioning System (GPS). From the controller design standpoint, several techniques such as LQR, H_∞, and multiple-model switching have been used in the DS formation control.

2.2.2 Virtual Structure

The virtual structure (VS) architecture considers all vehicles as rigid bodies embedded in a large virtual body. The whole motion of the VS system takes each individual vehicle's motion into account in order to determine the whole rigid body motions. There are two types of virtual structures: iterated VS (IVS) and guidance VS (GVS) [2]. This will be described in more details next.

In IVS, a special formation template (structure) is obtained for the present position of each vehicle at any point in time. Then, each vehicle considers the resultant special formation as a reference to track its desired position. The state of each vehicle depends on the corresponding special formation at any point in time. Different templates are introduced for different objectives in the literature. For example, an algorithm is proposed in [12] to find a "so called" *virtual center*. The virtual center is then treated as a virtual leader to reduce the tracking errors. The main advantage of the virtual center approach is that it can indicate the weighted average motion of each vehicle.

GVS, on the other hand, was introduced in [13] as a constellation template for

each vehicle. The template was to keep the desired relative position and orientation of each vehicle with respect to a constellation coordinate system.

2.3 Formation Flying of UAVs

As mentioned before, a considerable amount of research has been carried out in the area of UAV formation flying; e.g., in the field of optimal fuel-cost, optimal energy, and optimal mission time. Several applications are also investigated in the literature. For example, forest fire detection by means of low attitude short endurance (LASE) UAVs was investigated in [4], where a new method was proposed to detect the exact perimeter of the fire range with a minimized mission time. The method aimed to solve the tracking problem in a real-time fashion. Since the fire range can be very large in practice, only one UAV may not accomplish the monitoring mission by itself within a reasonable period of time. Four to six UAVs working as a team was proposed in [4] for this objective.

To achieve higher quality images, LASE UAVs were used in [4]. A new algorithm was also developed to increase the flexibility in employing LASE UAVs, in this case. This algorithm has several advantages. First of all, it is capable of adding or removing UAVs from the team. Secondly, it can be deployed to monitor the change in fire pattern. The third advantage is that it is suitable for the missions that require to be accomplished rapidly. This class of missions includes fire detection.

An optimal fuel-cost approach was introduced for formation flying in [18]. The method was based on minimizing the following fuel-cost function:

$$J = \sum_{i=1}^{K} \sum_{p=1}^{N} \sum_{j=1}^{n_u} r_{ij} |u_{ipj}| \tag{2.2}$$

where r_{ij} denotes the weight coefficient and u_{ipj} is the jth component of the input vector of vehicle i at the pth time step. Note that equation (2.2) is, in fact, a discrete approximation for the continuous-time fuel-cost differential equation [18]. Some important constraints should also be taken into consideration in practice, and as a result, the problem turns out to be a constrained optimization problem as formulated below:

$$\min J = \sum_{i=1}^{K} \sum_{p=1}^{N} \sum_{j=1}^{n_u} r_{ij} |u_{ipj}| \tag{2.3}$$

subject to:

$$|u_{ipj}| \leq v_{ipj},$$

where v_{ipj} is a positive variable whose value depends on the actuator's mechanism and their limitations [18].

Let the translational velocity be given by:

$$v_i^2 = \dot{x}_i^2 + \dot{y}_i^2 \tag{2.4}$$

Then the cost function (2.3) can approximately be rewritten as:

$$\min J = \sum_{i=1}^{K} \sum_{p=1}^{N} v_{ip1} + v_{ip2} \tag{2.5}$$

subject to:

$$|\dot{x}_{ip}| \leq v_{ip1},$$

$$|\dot{y}_{ip}| \leq v_{ip2}$$

One can use the existing softwares to solve the optimization problem given above, with the corresponding linear constraints on maximum allowable control magnitude, collision avoidance, obstacle avoidance, etc. The results, however, may be an approximation to the exact optimal fuel-cost trajectory for each UAV [18].

The idea of using hierarchical control system analysis in optimal formation flying of UAVs was first introduced in [34], where a two-layer hierarchical control system was proposed to handle the required information flow for control. This, in fact, leads to the minimum time solution for a square formation. In other words, it provides a control strategy to create a square formation for four UAVs as quickly as possible. To obtain the corresponding optimal control strategy, the upper layer considers the trajectory in X and Y directions, separately. Then, the lower layer will use this trajectory.

At the top layer, the following cost function is to be minimized:

$$J = \int_{t_0}^{t_f} (1 + 0.5u^T R_{top} u) dt \tag{2.6}$$

where t_0 and t_f denote the initial time and final time, respectively, and R_{top} is a positive definite matrix which determines the relative importance of mission time versus input energy. It is to be noted that when R_{top} is very small, the minimized result obtained is a solution for minimum time mission. At the lower layer, on the other hand, the following cost function

is considered:

$$J = 0.5 \int_{t_0}^{t_f} [(x_t - C_a x_l)^T Q_{low} (x_t - C_a x_l) + (u_t - D_a u_l)^T R_{low} (u_t - D_a u_l)] dt \qquad (2.7)$$

subject to:

$$\dot{x_l} = A_l x_l + B_l u_l$$

where Q_{low} and R_{low} represent the weighting matrices for the tracking error and input energy, respectively, and A_l and B_l are the state-space matrices which specify the desired trajectory. Moreover, the matrices C_a and D_a in (2.7) are given by:

$$C_a = \begin{bmatrix} C_1 & C_2 & 0 & 0 \\ 0 & C_1 & C_2 & 0 \\ 0 & 0 & C_1 & C_2 \end{bmatrix}$$

$$D_a = \begin{bmatrix} 1 & 0 & -1 & 0 & & & & \\ 0 & 1 & 0 & -1 & & & & \\ & & 1 & 0 & -1 & 0 & & \\ & & 0 & 1 & 0 & -1 & & \\ & & & & 1 & 0 & -1 & 0 \\ & & & & 0 & 1 & 0 & -1 \end{bmatrix}$$

where C_1 =diag $(1,1,1,1)$ and C_2 =diag $(-1,-1,-1,-1)$.

Optimal control theory was then used to obtain the best trajectory with respect to the cost function (2.6) and (2.7) for the square formation with constant speed. Simulation results presented in [34] show promising results. However, this algorithm has the following

shortcomings: First, it is only suitable for formations with four UAVs; second, it only considers square formation, not any general one.

An optimal formation flying strategy was proposed in [24] to minimize the required energy for the reconfiguration of multiple spacecraft. The approach was based on splitting the trajectory of the spacecraft into a set of way-points in order to obtain an optimal law which also guarantees collision avoidance. Furthermore, a numerical algorithm was given in [24] to solve the optimization problem efficiently. This algorithm consists of two main components:

1. **DIG** algorithm to separate all vehicles for collision avoidance (details of DIG algorithm are discussed in [24]);

2. **JG** algorithm to minimize the following cost function:

$$J_\mu = \sum_{l=1}^{N} \mu_l \int_0^T a_l^T(t) a_l(t) dt \tag{2.8}$$

Note that any other optimization algorithm can alternatively be used instead of **JG** algorithm to solve equation (2.8) . Although the technique proposed in [24] considers formation of a group of spacecraft, it can be extended to UAVs.

Chapter 3

Minimum Time Strategy for Formation Reconfiguration

The main objective in this chapter is to obtain a proper transition strategy for UAV formation switching. It is assumed that a set of desired formation structures is given. In many practical applications, the transition strategy when UAVs change formation is based on minimum fuel or minimum energy performance. There are, however, several applications where due to the nature of the mission, the time factor is of a crucial importance. In this chapter different strategies for minimum time formation reconfiguration will be studied and it will be shown that the proposed strategy can result in a significant reduction in the time for reconfiguration with a rather small increase in the power required, in practice. The results obtained can be applied to formations with any architecture such as leader/follower

(L/F) and virtual structure (VS) architectures.

3.1 Formation Transition

3.1.1 Problem Definition

Some important definitions will be introduced now, which will be referred to later in the main results.

- **Idle time:** The time interval between the accomplishment of one mission and issuance of the command for the next mission will be referred to as idle time.
- **SD formation:** A special designated formation which is close to all possible formations. This formation is essential in the main development of this work.
- Two different approaches will be studied in this chapter.

  Approach 1: UAVs will keep flying in their current formation during the idle time till they receive the command to fly to next formation.

  Approach 2: UAVs will fly to the SD formation during the idle time and will move to the next formation when they receive new missions commands.

- **Leader Frame:** The leader UAV will be regarded as the origin of the reference frame

for relative positions and velocities. The x-axis of the frame is directed towards the leader's head, as shown in Figure 3.1. In this frame, all locations of formations are fixed. Note that the velocity of the leader measured in this frame is zero.

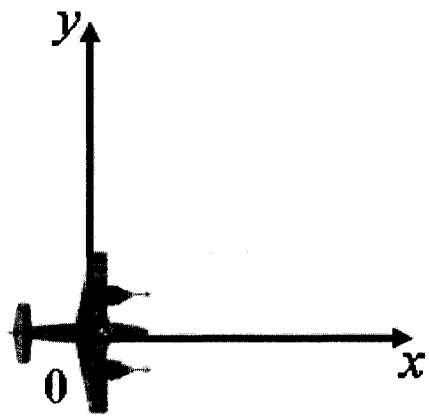

Figure 3.1: The leader-frame with a 2-D model

- The overall distance between the current location for each UAV and all possible locations given by the set of formations is denoted by d_p, as follows: $d_p = \sum_{k=1}^{L-1} |\vec{d}_{j(k)j(k+1)}|$, $j(k) \in$ S, where S represents a special scenario given by mission commands and is characterized by a sequence. L is the size of the sequent set S. For instance, the size of the sequent set $S = (1,2,3,4,3,2,1)$ is equal to 7. $j(k)$ denotes the values chosen from the sequent set S in a prescribed order. To clarify the above discussion, consider the sequent set $S = (1,2,3,4,3,2,1)$. One can easily verify that for this case: $d_p = |\vec{d}_{12}| + |\vec{d}_{23}| + ... + |\vec{d}_{21}|$. **Note:** $j(1)$ is assumed to represent the initial formation.

- The overall distance between the location of SD formation and all possible locations

given by the set of formations is denoted by d_0, and can be obtained as follows:

$$d_0 = \sum_{k=1}^{L-1} |\vec{d}_{0j(k+1)}|, j(k) \in \mathrm{S}$$

- $\vec{V}_{j(k)j(k+1)}$ is the relative velocity from location $j(k)$ to location $j(k+1)$ measured in the leader frame.

- $\vec{V}_{0j(k+1)}$ represents the relative velocity from the location of SD formation to the location number $j(k+1)$ in S, measured in the leader frame.

- $\vec{V}_l$ is the velocity of the leader measured in the Earth frame. It is a constant value when UAVs change their formations. In other words, the leader will have a cosntant speed during the transitional period of UAVs from one formation to another.

- $\vec{V}_{max}$ denotes the maximum velocity of UAVs measured in the Earth frame.

- $t_p = \sum_{k=1}^{L-1} \frac{|\vec{d}_{j(k)j(k+1)}|}{|\vec{V}_{j(k)j(k+1)}|}$ represents the mission time of the sequent set S corresponding to Approach 1.

- $t_0 = \sum_{k=1}^{L-1} \frac{|\vec{d}_{0j(k+1)}|}{|\vec{V}_{0j(k+1)}|}$ is the mission time of the sequent set S corresponding to Approach 2.

3.1.2 Assumptions

The following assumptions are required in the development of the main results.

1. A set of desired configurations for the formation of the UAVs is given as *a priori* information. However, the order of switching from one configuration to another is unknown.

2. The idle time is sufficiently long, or more precisely, it is at least twice as long as the settling time (within a certain percentage of the steady-state) of the overall formation control system.

3. All UAVs have the same dynamics.

4. Each UAV control unit operates independently of the other ones.

5. All configurations in the known finite set are convex (in terms of the geometric shape).

3.1.3 Problem Statement

Suppose there are N UAVs which can create M different formations by random orders (N and M are finite). It is desired to find a special designated formation (SD formation) for UAVs, which they should fly to, between any two consecutive formation commands (within the idle time). The main purpose of defining this designated formation is to stay close to all possible locations that they may require to move to, upon receiving the next mission command. The ultimate objective is to minimize the reconfiguration time. In other words, the SD formation is a transition bridge between all possible formations. Upon the

completion of a mission and before the issuance of a new formation command (i.e., during the idle time), the UAV will fly to the SD formation. This formation has the property that can minimize the transition time due to its closeness to the next potential locations.

For any given formation, let T and T_i denote the time it takes for all UAVs to change their position, and the time it takes for the ith UAV to change its position according to the new command, respectively. T is, in fact, the mission time for all UAVs while T_i represents the mission time for the ith UAV. The main objective can now be described in terms of the above parameters as follows:

Problem 1: Find the SD formation such that if all UAVs fly to their positions in this formation and stay there during the idle time, then the resultant mission time T is minimized.

It is desired now to translate the problem of finding SD formation (or at least a formulation for it) using simple mathematical and physical concepts. First of all, according to Assumption 4 all UAVs operate independently when they change formations. Since all of the UAVs are assumed to have the same dynamics (according to Assumption 3), one can find the SD position for each UAV separately. In other words, the SD formation is indeed the combination of all SD positions obtained for each individual UAV. This idea can be easily used for any formation flying structure, e.g. L/F FFC, MIMO FFC, and VS FFC, in order to achieve fast missions.

Consider now N UAVs with a given set of M formations, and suppose that the location and the orientation of each UAV in each formation is known. Let the position of one arbitrary UAV in the jth formation be denoted by $l(x_j, y_j, z_j)$, $j \in$ M, in 3D space. Position of this UAV in the SD formation is represented by $l(x_0, y_0, z_0)$. It is desired to find the SD position for all UAVs.

Assume that the magnitude of the velocity of each UAV remains approximately constant at all times (this is a realistic assumption in many formation applications [35], [22]). This implies that the acceleration of each UAV is sufficiently small at any point in time, and hence the mission time is proportional to the distance d. As a result, the minimum time problem turns out to be equivalent to the minimum distance problem, which can be formulated for each UAV as follows:

$$\min(d = \sum_{j=1}^{M} \Delta_j) \tag{3.1}$$

where $\Delta_j = \sqrt{(x_j - x_0)^2 + (y_j - y_0)^2 + (z_j - z_0)^2}$

The following set of partial derivatives can be utilized to solve the equation (3.1) for x_0, y_0, and z_0.

$$\begin{cases} \frac{\partial d}{\partial x_0} = \sum_{j=1}^{M} \frac{(x_j - x_0)}{\Delta_j} = 0 \\ \frac{\partial d}{\partial y_0} = \sum_{j=1}^{M} \frac{(y_j - y_0)}{\Delta_j} = 0 \\ \frac{\partial d}{\partial z_0} = \sum_{j=1}^{M} \frac{(z_j - z_0)}{\Delta_j} = 0 \end{cases} \tag{3.2}$$

The problem is now converted to finding the conditions under which the equation

(3.2) has at least one solution. Mathematically, there exists at least one solution for the equation (3.1) when the corresponding M points for each UAV form a convex shape [36], [37]. Although by assumption this condition holds, it is very difficult to find an analytical solution for this problem. Hence, a proper approach will be given next to tackle the problem.

3.1.4 Basic Solutions

Consider M points in a three dimensional space, represented by P_1, P_2, ..., P_M. The problem is to find a point P_0 such that the total distance from the above points to P_0 is the minimum possible value. In other words, the point P_0 can minimize the sum $z = \sum_{j=1}^{M} \|P_{j0}\|$, where P_{j0} represents a vector from P_j to P_0, $j \in 1,2,...,M$. The solution of this problem is the solution of the equation (3.1) too. This turns out to be the *Fermat-Torricelli Problem* which is a well-known problem in geometry, and the solution(s) is (are) called *Fermat-Torricelli Point(s)*, and throughout this thesis will simply referred to as Fermat Point(s).

The Fermat Point is a well-know problem in mathematics. This problem was initiated by Pierre de Fermat in 1643, as a question in a letter, which was *to find a point having the minimal sum of distances to three given points in the plane.* E.Torricelli gave the initial solution of the problem. This problem is called "Fermat problem" or "Fermat-Torricelli problem", and the corresponding point is often referred to as "Fermat Point", "Fermat-Torricelli Point", and "Weber Point".

The exact location of the Fermat Point can be obtained analytically, but involves sophisticated equations when the number of points is greater than four. In such cases, a numerical solution or an approximate location of the Fermat point would be more desirable. In the special case of three points ($M = 3$), on the other hand, the problem is solved analytically in [38] and [39], and the solution is referred to as **First Fermat Point**. First Fermat Point has the following properties:

- If no angle of the triangle $\triangle P_1P_2P_3$ is greater than 120^o, the Fermat Point P_0 belongs to the interior of the triangle and satisfies $\angle P_1P_0P_2 = \angle P_2P_0P_3 = \angle P_3P_0P_1 = 120^o$.
- If any of the angles of the triangle $\triangle P_1P_2P_3$ is greater than or equal to 120^o, the vertex of that angle will be the First Fermat Point (the vertex of the obtuse angle). For example, if $\angle P_1P_2P_3 \geqslant 120^o$, then the point P_2 is the First Fermat Point.

The following proposition gives the exact Fermat Point for four points.

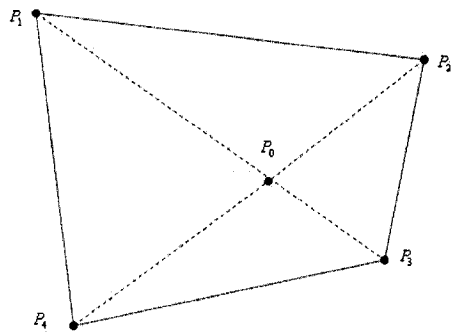

Figure 3.2: The Fermat Point for 4 convex points

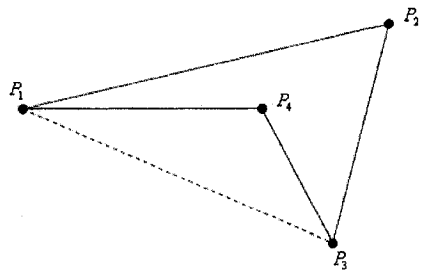

Figure 3.3: The Fermat Point for 4 non-convex points

Proposition 1 Consider four points P_1, P_2, P_3, and P_4, in two dimensional space $\mathbb{R}^2$.

(i) The Fermat Point will be the intersection of the two diagonals if the four points create a convex shape;

(ii) The Fermat Point will be the vertex that is inside of the triangle formed by the other three points if the four points create a non-convex shape.

Proof:

Case (i): Assume that the four points form a convex quadrilateral (all interior angles are less than 180^o). Let P_0 denote the intersection of the two diagonals of the quadrilateral, and P_5 be an arbitrary point on the plane, as shown in Figure 3.4. It is desired to show that the following inequality holds:

$$\sum_{j=1}^{4} \|P_j P_0\| \leqslant \sum_{j=1}^{4} \|P_j P_5\| \tag{3.3}$$

where $\|\cdot\|$ denotes the Euclidean Norm. Note that:

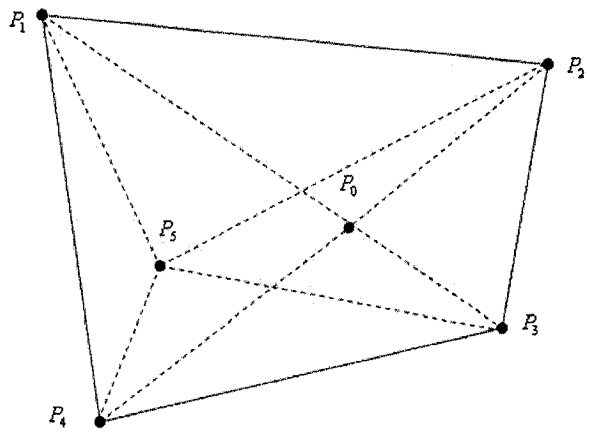

Figure 3.4: Four points forming a convex shape

$$\begin{cases} \|P_1P_0\| + \|P_3P_0\| = \|P_1P_3\| \\ \|P_2P_0\| + \|P_4P_0\| = \|P_2P_4\| \end{cases} \tag{3.4}$$

Now, it can be easily verified that:

- If P_5 is not on the line $\overline{P_1P_3}$, then $\|P_1P_5\| + \|P_3P_5\| > \|P_1P_3\|$.
- If the point P_5 is on the line $\overline{P_1P_3}$, then $\|P_1P_5\| + \|P_3P_5\| = \|P_1P_3\|$.

Similarly:

- If P_5 is not on the line $\overline{P_2P_4}$, then $\|P_2P_5\| + \|P_4P_5\| > \|P_2P_4\|$.
- If the P_5 is on the line $\overline{P_2P_4}$, then $\|P_2P_5\| + \|P_4P_5\| = \|P_2P_4\|$.

Now, If the point P_5 is not the intersection of the lines $\overline{P_1P_3}$ and $\overline{P_2P_4}$, the following inequality holds:

$$\|P_1P_3\| + \|P_2P_4\| < \|P_1P_5\| + \|P_2P_5\| + \|P_3P_5\| + \|P_4P_5\| \tag{3.5}$$

which implies that:

$$\sum_{j=1}^{4} \|P_jP_0\| < \sum_{j=1}^{4} \|P_jP_5\| \tag{3.6}$$

Case (ii): Assume now that the four points form a concave quadrilateral in 2D space (one interior angle is greater than 180^o), where the point P_4 is the vertex inside $P_1P_2P_3$. Choose an arbitrary point P_5 in the space and draw straight lines from it to all four points, as shown in Figure 3.5. Let the point P_x represent the intersection of the line $\overline{P_1P_5}$ and the extended line $\overline{P_3P_4}$. The following inequality holds

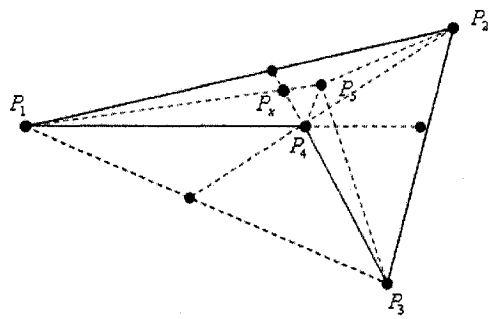

Figure 3.5: The Four points forming a convex shape

$$\|P_2P_4\| < \|P_4P_5\| + \|P_2P_5\| \tag{3.7}$$

On the other hand, the inequality $\|P_1P_4\| < \|P_1P_x\| + \|P_xP_4\|$ and $\|P_3P_4\| + \|P_4P_x\| < \|P_3P_5\| +$

$\|P_xP_5\|$ hold in the triangle $\triangle P_1P_xP_4$ and $\triangle P_3P_5P_x$, respectively. Combine these two inequalities to obtain:

$$\|P_3P_4\| + \|P_4P_x\| + \|P_1P_4\| < \|P_3P_5\| + \|P_xP_5\| + \|P_1P_x\| + \|P_xP_4\|$$

$$\Rightarrow \|P_3P_4\| + \|P_1P_4\| < \|P_3P_5\| + \|P_xP_5\| + \|P_1P_x\|$$

$$\Rightarrow \|P_1P_4\| + \|P_3P_4\| < \|P_1P_5\| + \|P_3P_5\| \tag{3.8}$$

Now, combine (3.7) and (3.8) to arrive at:

$$\|P_1P_4\| + \|P_2P_4\| + \|P_3P_4\| < \|P_1P_5\| + \|P_2P_5\| + \|P_3P_5\| + \|P_4P_5\| \tag{3.9}$$

Any other arbitrary point such as the points located on the lines $\overline{P_1P_4}$, $\overline{P_2P_4}$, and $\overline{P_3P_4}$ or their extended lines, will lead to a similar result. This means that the point P_4 is the Fermat Point for vertices of the concanve quadrilateral. This completes the proof. ■

It is to be noted that a different approach is given in [40] based on the contraction point of four points in $\mathbb{R}^2$, (in that work, Fermat Point is referred to as Weber Point)

It is very difficult to find the Fermat Point for more than five non-collinear points. Many researchers have worked in this area for the past several years and several relevant results are available in the literature. For example, the existence conditions for the Fermat Point and an analytical solution to find the Fermat Point in the $\mathbb{R}^d$ Euclidean space are provided in [36]. Furthermore, conditions for the existence of Fermat Point for a finite set of points in compact metric topological spaces are presented in [37]. It is also shown in [37] that if the points in the given finite set do not lie on the same line, then the Fermat

Point would be unique. This statement can be easily concluded from the equation (3.1), as well.

As mentioned earlier, an analytical solution for Fermat Point as a closed-form formula can be very cumbersome, in general. However, one can use various scientific softwares to find Fermat Point numerically. For instance, the function *fminsearch* on MATLAB which uses Nelder-Mead's direct search simplex method, can be utilized to obtain Fermat Point. However, the result obtained may be a local solution (as opposed to the global one) in the domain of attraction of the initial point used in the numerical procedure.

3.2 Probabilistic Set of Possible Formations

In this section, it is desired to extend the results obtained in the preceding section, to the case when different configurations in the given finite set have different probabilities assigned to them. In other words, it has been implicitly assumed so far in the development of the results that the probability of all different configurations in the given set is equal to $1/M$, where M is the size of the set (i.e., number of possible configurations). The fundamental issue which motivates this analysis is that in certain missions some of the configurations are known in advance to be called by the mission more frequently compared to the other ones. In such cases, the optimal location of the UAVs during the idle time will depend not only on their positions in the given set, but also on how frequently they are required to move

to those positions (which reflect, in fact, the corresponding probabilities). The statistical information about different configurations in the set will be considered as *a priori* data in what follows. Let the probability that the jth configuration is desired to be created by the UAVs be denoted by q_j. The problem of finding a location for each UAV to move to during the idle time can be formulated by equation (3.1) or equation (3.2). Now, to incorporate probabilities, equation (3.1) can be rewritten in the following form:

$$\min d = \sum_{j=1}^{M} q_j \Delta_j \tag{3.10}$$

The following partial derivatives can be used to solve (3.10):

$$\begin{cases} \frac{\partial d}{\partial x_0} = \sum\limits_{j=1}^{M} \frac{q_j(x_j - x_0)}{\Delta_j} = 0 \\ \frac{\partial d}{\partial y_0} = \sum\limits_{j=1}^{M} \frac{q_j(y_j - y_0)}{\Delta_j} = 0 \\ \frac{\partial d}{\partial z_0} = \sum\limits_{j=1}^{M} \frac{q_j(z_j - z_0)}{\Delta_j} = 0 \end{cases} \tag{3.11}$$

Similarly, MATLAB function *fminsearch* can find practical solutions. In the next section, an analytical solution is given for the case when one of the configurations has a probability greater than 0.5.

3.2.1 Fermat Point with Unequal Probabilities

Proposition 2 Let the set of M candidate points for an arbitrary UAV in the formation be given by P_j, $j \in \bar{\mathrm{M}} := \{1, \ldots, M\}$. Assume that a set of constant coefficients q_j, $j \in \bar{\mathrm{M}}$ is also given, where q_j denotes the probability that P_j is the desired position for this UAV any

time a reconfiguration command is issued. If the probability q_i of the point P_i satisfies the inequality $q_i \geq 0.5$ for an $i \in \bar{\mathrm{M}}$, then the point P_i is, in fact, the position of this UAV in the SD formation.

Proof: Since $\|P_iP_i\| = 0$, one can write:

$$\sum_{j=1}^{M} q_j \|P_jP_i\| = \sum_{\substack{j=1 \\ j\neq i}}^{M} q_j \|P_jP_i\|$$

where $\|\cdot\|$ denotes the Euclidean Norm. Choose an arbitrary point P_0, distinct from P_i in the set of candidate positions. Thus, the overall distance (weighted by the probabilities) between P_0 and all other candidate positions is:

$$d = \sum_{j=1}^{M} q_j \|P_jP_0\| \tag{3.12}$$

Furthermore, one can easily verify that

$$q_i \geq 0.5 \Longleftrightarrow q_i \geq \sum_{\substack{j=1 \\ j\neq i}}^{M} q_j$$

Define:

$$\Delta q := q_i - \sum_{\substack{j=1 \\ j\neq i}}^{M} q_j$$

(note that $\Delta q \in [0, 1]$). Now, from (3.12) and Δq:

$$\begin{aligned} d &= q_i\|P_iP_0\| + \sum_{\substack{j=1 \\ j\neq i}}^{M} q_j \|P_jP_0\| \\ &= \sum_{\substack{j=1 \\ j\neq i}}^{M} q_j \|P_iP_0\| + \Delta q\|P_iP_0\| + \sum_{\substack{j=1 \\ j\neq i}}^{M} q_j \|P_jP_0\| \\ &= \sum_{\substack{j=1 \\ j\neq i}}^{M} q_j (\|P_iP_0\| + \|P_jP_0\|) + \Delta q\|P_iP_0\| \end{aligned}$$

On the other hand, it is known that $\|P_iP_0\| + \|P_jP_0\| \geq \|P_jP_i\|$ for all $i, j \in \bar{\mathrm{M}}$. This, along with the inequality $\Delta q(\|P_iP_0\|) \geq 0$ implies that:

$$\sum_{j=1}^{M} q_j \|P_jP_i\| \leq \sum_{j=1}^{M} q_j \|P_jP_0\| \qquad \blacksquare$$

Remark 1: Throughout the development of the main result, the travel time of each UAV is considered proportional to its displacement. This means that it is implicitly assumed that the UAVs fly with a constant velocity. While this implicit assumption simplifies the problem formulation and its solution, we have obtained promising preliminary results for the case when the UAVs fly with nonzero acceleration. As a matter of fact, a constant nonzero acceleration is considered in the simulation results presented in the next section.

Remark 2: As a more general case, one can consider a compact set of candidate positions instead of a finite set, and a probability density function corresponding to the points in the compact set.

Remark 3: The idle time defined in this thesis should be long enough so that all UAVs can fly to their location in the SD formation and settle there, and then fly to their next position determined by the new reconfiguration command, and settle there too. This implies that the idle time must be at least twice as big as the settling time of the formation control.

3.2.2 Applications Of Two Dimensional Dynamics

Consider a set of UAVs whose dynamics is governed by the equation (2.1) in $\mathbb{R}^2$. As discussed before, it is assumed that the set of desired configurations for the formation of the UAVs is given as *a priori* information. Therefore, the location of SD formation for any UAV can be derived from equation (3.2) or equation (3.11). It is desired now to consider the effect of velocity component in the development. Generically, the inequality $d_0 < d_p$ holds, as a property of Fermat Point (there are some special cases, however, for which $d_0 \geqslant d_p$, as will be discussed later).

The relationship between the velocity and mission time will now be investigated. Defining times t_0 and t_p (defined in subsection (3.1.1)) for varying velocity and different configurations can be cumbersome, in general. Thus, it is more desirable to compare the maximum t_0 and the minimum t_p. In other words, the mission time corresponding to the worst case scenario for Approach 2, will be compared with the mission time corresponding to the best scenario for Approach 1. Hence, if the largest value of t_0 is less than the smallest value of t_p, the proposed approach is guaranteed to be superior over the traditional reconfiguration strategy.

Assume that the leader frame does not rotate in $\mathbb{R}^2$. Assume also that all UAV

followers will apply the maximum velocity (measured in the Earth frame) during the formation reconfiguration. Then:

$$|\vec{V}_{max}| - |\vec{V}_l| \leqslant |\vec{V}_{j(k)j(k+1)}| \leqslant |\vec{V}_{max}| + |\vec{V}_l| \tag{3.13}$$

$$|\vec{V}_{max}| - |\vec{V}_l| \leqslant |\vec{V}_{0j(k+1)}| \leqslant |\vec{V}_{max}| + |\vec{V}_l| \tag{3.14}$$

This results in:

$$min(t_p) = \frac{d_p}{|\vec{V}_{max}| + |\vec{V}_l|} \tag{3.15}$$

$$max(t_0) = \frac{d_0}{|\vec{V}_{max}| - |\vec{V}_l|} \tag{3.16}$$

Now, the inequality $max(t_0) < min(t_p)$ holds, if:

$$\frac{d_0}{|\vec{V}_{max}| - |\vec{V}_l|} < \frac{d_p}{|\vec{V}_{max}| + |\vec{V}_l|} \tag{3.17}$$

From the inequality (3.17) and the relation $d_p = \alpha \times d_0$, $\alpha > 1$, one can find the following conditional boundary for the maximum velocity:

$$|\vec{V}_{max}| > \frac{\alpha + 1}{\alpha - 1}|\vec{V}_l| \tag{3.18}$$

The inequality (3.18) can be rewritten as follows:

$$|\vec{V}_{max}| > \frac{d_p + d_0}{d_p - d_0}|\vec{V}_l| \tag{3.19}$$

which gives the sufficient boundary.

It is to be noted that the boundary condition given above provides a sufficient condition only for the proposed method to outperform the traditional reconfiguration strategy. In other words, t_0 can be less than t_p even when $|\vec{V}_{max}| \leqslant \frac{d_p+d_0}{d_p-d_0}|\vec{V}_l|$. Furthermore,

normally, the UAV does not reach its maximum velocity in a practical framework. Moreover, the results obtained above are based on the assumption that the leader frame does not rotate. This inequality may not hold for more complex dynamic equations, e.g., nonzero acceleration and rotation for UAVs.

Example 1 This example aims to demonstrate the conservativeness of the results obtained above. Consider two UAVs, one leader and one follower, flying in formation. Assume that these two UAVs are desired to create three different formations. The special scenario for the follower is given by S =(3,3,2,1), where the locations for the follower are $(0, 1000)$, $(1000, 1000)$, and $(1000, 0)$, respectively as shown in Figure 3.6. It is assumed that $|\vec{V}_l| = 5m/s$ (similarly to [41]). According to this scenario, the follower starts from formation #3, and then reconfigures to the formations 3, 2, and 1, sequentially. It will be moving with the maximum velocity during the reconfiguration. The SD formation in this case is located at the point **0**, as shown in Figure 3.6 .

The boundary condition for the given values in this example is $|\vec{V}_{max}| > \frac{d_p+d_0}{d_p-d_0}|\vec{V}_l| = 288.28m/s$ to get $t_0 < t_p$. However, it can be easily verified that a velocity as high as $|\vec{V}_{max}| = 60m/s$ will also yield $t_0 < t_p$. This shows the condition $|\vec{V}_{max}| > \frac{d_p+d_0}{d_p-d_0}|\vec{V}_l|$ can be very conservative, in general.

Example 2 Consider two UAVs, flying in a L/F formation structure. Three formations are designed to be generated, which are given by the points $P_1(0, 1000)$, $P_2(1000, 1000)$,

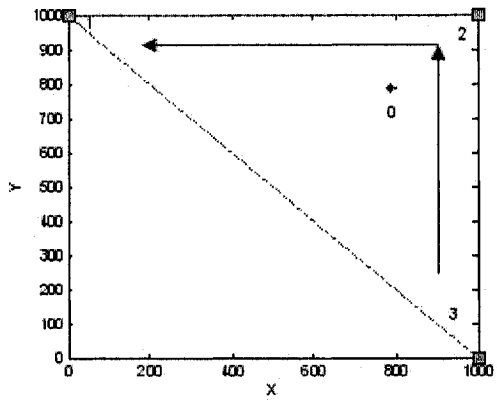

Figure 3.6: The reconfiguration scenario for Example 1

and $P_3(500,0)$ for the follower. Assume that $|\vec{V}_l| = 5m/s$ (just like the previous example). Consider the reconfiguration scenario S =(2,3,2,1,1), shown in Figure 3.7 .

If the probability assigned to P_1 in this example is $q_1 = 50\%$, according to Proposition 2 this point is, in fact, the position of the follower in the SD formation. Then, the boundary condition for this example is $|\vec{V}_{max}| > \frac{d_p+d_0}{d_p-d_0}|\vec{V}_l| = 92.796m/s$. However, in order for t_0 be smaller than t_p in this example, $|\vec{V}_{max}|$ is required to be greater than $65m/s$. This is approximately 70% of the boundary value obtained above, which represents a less conservative case compared to the previous example.

These two examples show that the boundary condition provides a sufficient condition, which depending on the parameters of the system such as formation scenarios and dynamic of UAV, it may lead to different levels of conservativeness. It is to be noted that

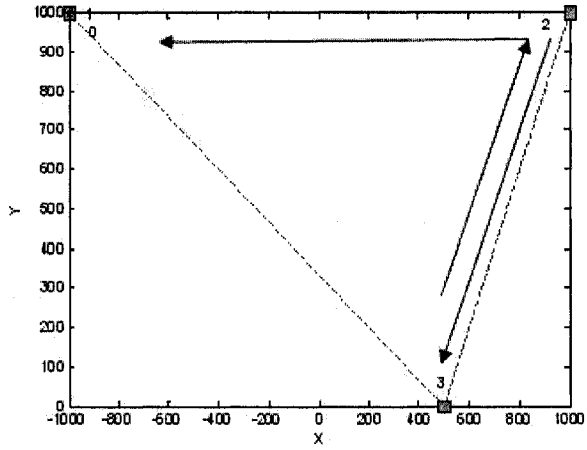

Figure 3.7: The reconfiguration scenario for Example 2

in many practical applications the speed of UAV does not exceed $36.11 m/s$ [41], which is typically much smaller than the boundary value for achieving $t_0 < t_p$.

3.2.3 Simulations

In this section, two examples will be presented to illustrate the effectiveness of the algorithm proposed in this thesis.

Example 3 In this example, three UAVs will similarly be used to create four different formations. UAV #1 is chosen as the leader and the other two UAVs, UAV #2 and 3 are treated as the followers. It is desired to create different configurations by positioning the followers properly, while the leader's position is considered to be fixed. Figure 3.8 shows the structures of four formations. Figure 3.9 shows the flying scenario when UAVs

applied the Approach 2.

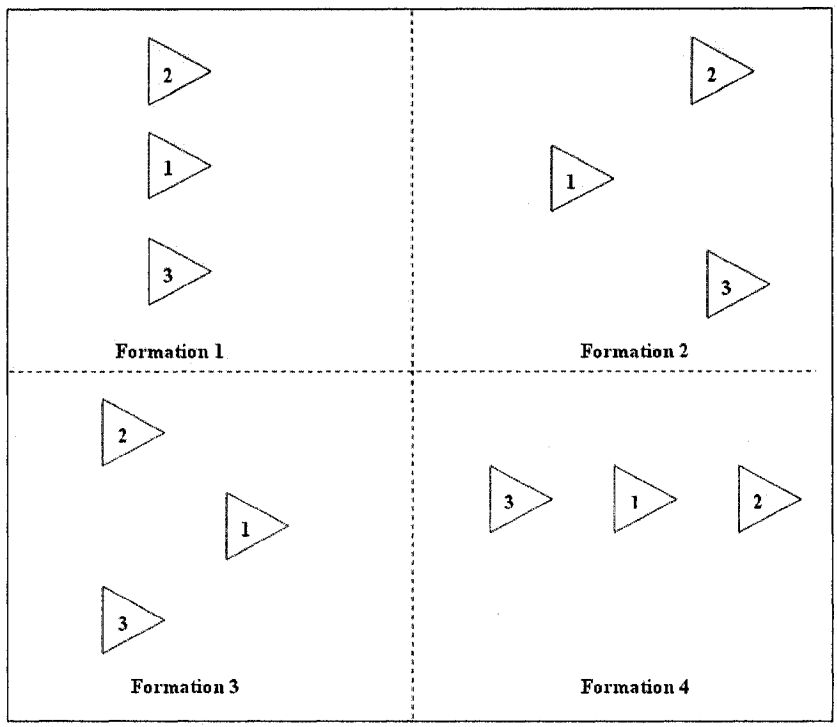

Figure 3.8: Formations configurations

The details of the potential configurations are as follows:

- The potential locations of the followers are given as: UAV #2 can move to one of the four points $P_{21}(0,1000)$, $P_{22}(1000,1000)$, $P_{23}(-1000,1000)$, and $P_{24}(1000,0)$ in the leader frame (Note that P_{ij} denotes the location of *ith* UAV at *jth* formation). UAV #3, on the other hand, can take one of the four spots $P_{31}(0,-1000)$, $P_{32}(1000,-1000)$, $P_{33}(-1000,-1000)$, and $P_{34}(-1000,0)$ (Note that for this particular case $N=3$ and $M=4$).

- The scenario for the followers to change position during the reconfiguration is S=(1,2,3,4,1).

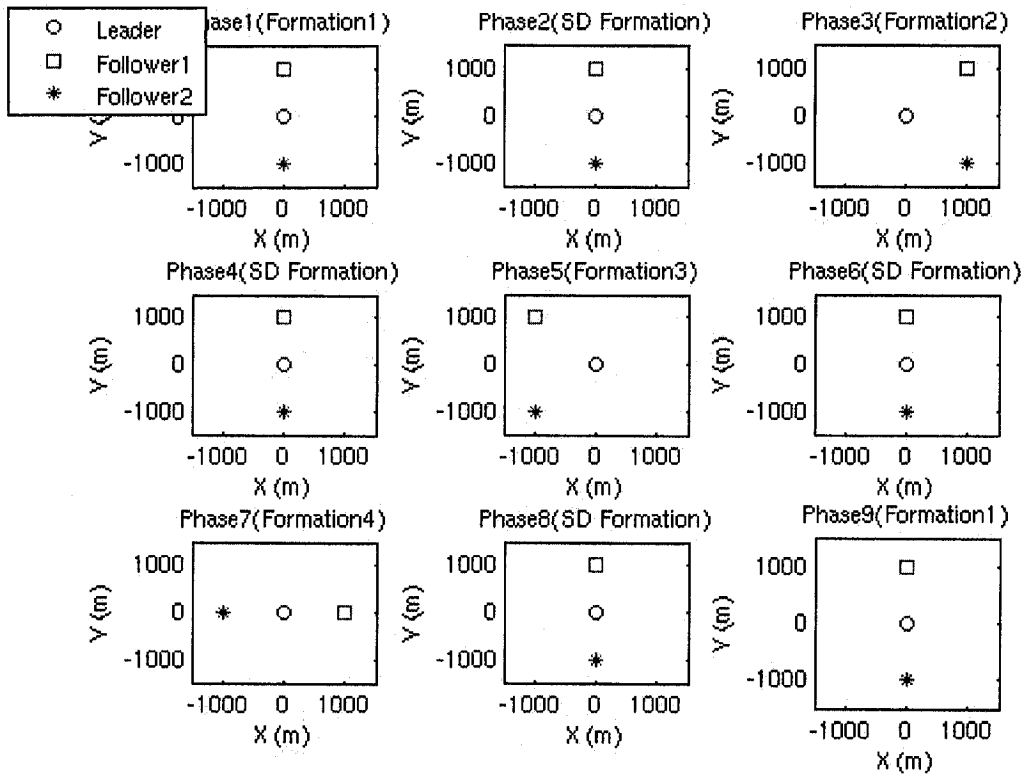

Figure 3.9: Formation flying scenario

This means that the formation starts from the first point (corresponding to the first configuration) and eventually switches to this state, after switching to configuration #2, 3, and 4, respectively.

- The idle time is assumed to be $90sec$, $130sec$, $150sec$, and $170sec$ when switching from configuration #1 to 2, 3, 4 and 1, respectively.

- The magnitudes of velocities V_l and V_{max} are $5m/s$ and $20m/s$, respectively. While the followers change their positions, the leader will keep its velocity constant at V_l. The followers will take the velocity V_{max} when they change their positions;

- Several assumptions are introduced here to obtain the results simply.

  1. The time of rolling and turning actions of UAVs are neglectable;
  2. The time for accelerating to V_{max} and decelerating to V_l are neglectable. In other words, it is regarded as constant velocity movement when UAVs switch their formations.

The relative time difference between Approach 1 and 2 is given by:

$$\Delta_{time} = \frac{(t_p - t_0)}{t_p} \tag{3.20}$$

Note that when Δ_{time} is positive, it implies that the proposed method, i.e. Approach 2, results in a faster mission. The power required of the UAV, on the other hand, can be obtained from the following equation [42], [43]:

$$P_A(\rho, \tau, V) = \left[\frac{C_{D0}\rho V^3}{2(W/S_w)} + C_{D0,L}V + \frac{2(W/S_w)}{\pi \ell R_A \rho V}\right] W \tag{3.21}$$

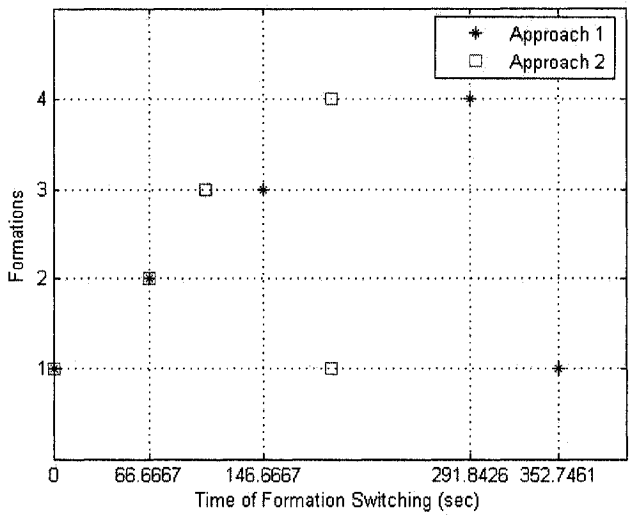

Figure 3.10: Reconfiguration history for UAV #2

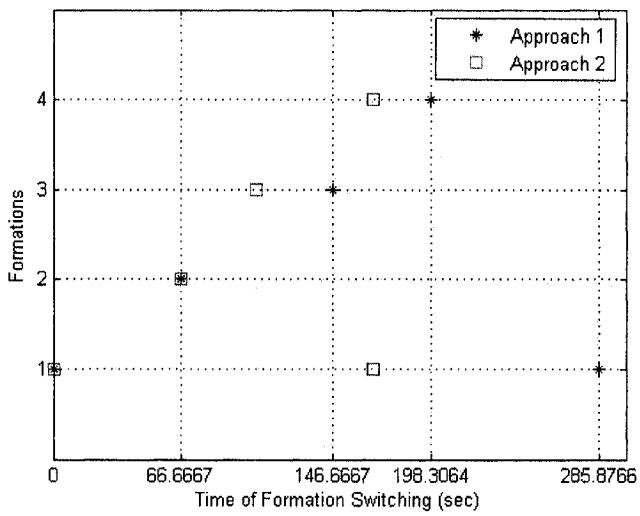

Figure 3.11: Reconfiguration history for UAV #3

The relative difference between power required corresponding to Approach 1 and 2 is then:

$$\Delta_{power} = \frac{(P_{Ap} - P_{A0})}{P_{Ap}} \tag{3.22}$$

Simulation results are given in Figure 3.10 and Figure 3.11, which show that by using the method proposed in this work, one can reduce the mission time by 45% (i.e., $\Delta_{time} = 45\%$) and 41.4% (i.e., $\Delta_{time} = 41.4\%$) for UAV #2 and #3, respectively, independently from the idle time (as long as it is sufficiently large so that the UAVs can settle down in their new position). Furthermore, using the proposed technique the power required of the UAVs can potentially be reduced in most of the cases. Table 3.1 summarizes the simulation results of power required for four different idle times.

UAV #2				UAV #3			
Idle Time	Approach 1	Approach 2	Δ_{power}	Idle Time	Approach 1	Approach 2	Δ_{power}
90sec	5.055	3.801	24.8%	90sec	4.129	4.271	-3.4%
130sec	5.130	3.513	31.6%	130sec	4.203	3.731	11.23%
150sec	5.167	3.532	31.6%	150sec	4.241	3.683	13.15%
170sec	5.205	3.717	28.6%	170sec	4.278	3.809	10.97%

Tabel 3.1: Power required for different idle times (unit: $(m * kg/s) * 10^{-5}$)

One can conclude from the above results that the proposed technique not only results in a faster reconfiguration, it also reduces the power required of both UAVs for idle times is equal to or greater than 130 sec. While in this work the analytical results are derived only for the mission time, reduction in the power required is due to the fact that normally the power required is closely related to the duration of the mission and the amount of power required to accomplish a long mission can potentially be high.

It is to be noted that the minimum time results given above rely on the assumption that the followers fly with a constant speed during the reconfiguration period; i.e., the acceleration is assumed to be zero (or approximately zero) throughout this development. It is also assumed that the leader frame maintains its original velocity during the transition period. These are realistic assumptions which are made in several papers as well; see, e.g. [35], [22]. Note also that the power required equation (3.21) is only valid for flying with no acceleration and at the same altitude.

Example 4 In this example, the formation consists of three UAVs: UAV #1 is the leader, and UAV #2 and #3 are followers. It is assumed that the magnitude of the initial velocity is $5m/s$, the magnitude of the maximum velocity is $20m/sec$ (both in the Earth frame). Upon the issuance of a reconfiguration command, the UAVs increase their speed from the initial value to the maximum value, and once the reconfiguration is accomplished, they reduce their speed to the initial value again (to save fuel). It is also assumed that only followers will change their positions to create the desired formations. The set of configurations for each UAV is given by three points; one for each configuration. These points are as follows (the position units are all meters): UAV #2: (0,1000), (1000,1000), and (1000,0); UAV #3: (0,-1000), (1000,-1000), and (-1000,0). Furthermore, suppose that the probability of the first configuration in 0.5 while the probability of each of the other two is 0.25. For this problem set-up, the locations of UAV #2 and #3 in the SD formation will be (0,1000) and (0,-1000), respectively. The idle time is assumed to be $70sec$ (Case 1) and $80sec$ (Case 2). All possible scenarios for formation switching are examined in the

simulations (36 different scenarios in this example). In general, the number of all possible scenarios can be obtained from the following equation (see Appendix A):

$$N_s = M_s * \frac{L!}{\prod_{l=1}^{k} Q_l!} \tag{3.23}$$

(the parameters M_s, L, and Q_l are defined in Appendix A). Δ_{avgT} and Δ_{avgP} are defined as follows:

$$\Delta_{avgT} = \frac{\sum_{i=1}^{N_s} \Delta^i_{time}}{N_s} \tag{3.24}$$

$$\Delta_{avgP} = \frac{\sum_{i=1}^{N_s} \Delta^i_{power}}{N_s} \tag{3.25}$$

Starting Point / Sequent	P_{21} [0,1000]	P_{22} [1000,1000]	P_{23} [1000,0]
1-3-2-1	179.21	219.21	240.11
1-3-1-2	215.14	255.14	276.04
1-1-3-2	139.21	179.21	200.11
1-1-2-3	118.31	158.31	179.21
1-2-3-1	179.21	219.21	240.11
1-2-1-3	194.24	234.24	255.14
2-1-3-1	255.14	188.47	240.11
2-1-1-3	194.24	127.57	179.21
2-3-1-1	179.21	112.54	164.18
3-1-2-1	255.14	219.21	167.57
3-1-1-2	215.14	179.21	127.57
3-2-1-1	179.21	143.28	91.64

Table 3.2: Reconfiguration time t_p for UAV #2 (unit: sec)

The mission times t_0 and t_p will be compared now. Note that the mission time was shown t_0 to be independent of the idle time, as long as it is sufficiently long. Thus, idle time will not be considered in the simulations here. The mission t_0 corresponding to Approach 2 will be $154.237sec$ and $127.57sec$ for UAV #2 and UAV #3, respectively. On

Starting Point / Sequent	P_{31} [0,-1000]	P_{32} [1000,-1000]	P_{33} [-1000,0]
1-3-2-1	246.08	286.08	333.65
1-3-1-2	215.14	255.14	302.71
1-1-3-2	206.08	246.08	293.65
1-1-2-3	158.51	198.51	246.08
1-2-3-1	246.08	286.08	333.65
1-2-1-3	167.57	207.57	255.14
2-1-3-1	255.14	188.47	333.65
2-1-1-3	167.57	100.9	246.08
2-3-1-1	246.08	179.41	324.59
3-1-2-1	255.14	286.08	194.24
3-1-1-2	215.14	246.08	154.24
3-2-1-1	246.08	277.02	185.18

Table 3.3: Reconfiguration time t_p for UAV #3 (unit: sec)

the other hand, the mission time t_p corresponding to Approach 1 is given in Tables 3.2 and 3.3 for UAV #2 and UAV #3, respectively. Furthermore, from equation (3.24) Δ_{avgT} for UAV #2 and UAV #3 are obtained to be 13.99% and 42.9%, respectively. This implies that using Approach 2, the average mission time for formation reconfiguration over all possible scenarios is reduced significantly for both UAVs.

Analogously, Δ_{avgP} for UAV #2 is obtained from equation (3.25) to be -11.8% in Case 1 and -3.2% in Case 2, respectively. Similarly, Δ_{avgP} for UAV #3 is equal to -10.6% and -0.2%, in Case 1 and Case 2, respectively. One can conclude from these results that Approach 2 will only cost 15% more power. As a matter of fact, the results given in Tables 3.4 and 3.11 show that Approach 2 can lead to a smaller power required in several scenarios. Note that positive Δ_{power} in these tables means that the power required for the corresponding scenario will be smaller using Approach 2.

Starting Point / Sequent	P_{21} [0,1000]		P_{22} [1000,1000]		P_{23} [1000,0]	
	Approach1	Approach2	Approach1	Approach2	Approach1	Approach2
1-3-2-1	2.6572	2.9395	3.2114	3.0077	3.5011	3.4997
1-3-1-2	3.155	2.8713	3.7093	2.9395	3.9989	3.4315
1-1-3-2	2.1029	2.8713	2.6572	2.9395	2.9468	3.4315
1-1-2-3	1.8132	2.3793	2.3675	2.4475	2.6572	2.9395
1-2-3-1	2.6572	2.9395	3.2114	3.0077	3.5011	3.4997
1-2-1-3	2.8654	2.3793	3.4196	2.4475	3.7093	2.9395
2-1-3-1	3.7093	2.9395	2.7855	3.0077	3.5011	3.4997
2-1-1-3	2.8654	2.3793	1.9416	2.4475	2.6572	2.9395
2-3-1-1	2.6572	2.9395	1.7334	3.0077	2.4489	3.4997
3-1-2-1	3.7093	2.9395	3.2114	3.0077	2.4959	3.4997
3-1-1-2	3.155	2.8713	2.6572	2.9395	1.9416	3.4315
3-2-1-1	2.6572	2.9395	2.1593	3.0077	1.4437	3.4997

Table 3.4: Power required of UAV #2 corresponding to Case 1

(unit: $(m * kg/s) * 10^{-5}$)

Starting Point / Sequent	P_{21} [0,1000]		P_{22} [1000,1000]		P_{23} [1000,0]	
	Δ_{time}	Δ_{power}	Δ_{time}	Δ_{power}	Δ_{time}	Δ_{power}
1-3-2-1	0.13935	-0.10625	0.2964	0.063441	0.35765	0.0004
1-3-1-2	0.28309	0.089929	0.39548	0.20753	0.44126	0.1419
1-1-3-2	-0.10794	-0.3654	0.13935	-0.10625	0.22925	-0.16447
1-1-2-3	-0.30371	-0.31218	0.025707	-0.033788	0.13935	-0.10625
1-2-3-1	0.13935	-0.10625	0.2964	0.063441	0.35765	0.0004
1-2-1-3	0.20593	0.16963	0.34153	0.28428	0.39548	0.20753
2-1-3-1	0.39548	0.20753	0.18165	-0.079755	0.35765	0.0004
2-1-1-3	0.20593	0.16963	-0.20904	-0.26055	0.13935	-0.10625
2-3-1-1	0.13935	-0.10625	-0.37047	-0.73514	0.06058	-0.42905
3-1-2-1	0.39548	0.20753	0.2964	0.063441	0.079569	-0.40218
3-1-1-2	0.28309	0.089929	0.13935	-0.10625	-0.20904	-0.76733
3-2-1-1	0.13935	-0.10625	-0.076475	-0.3929	-0.68308	-1.424

Table 3.5: Comperative results for mission time and power required for

UAV #2 corresponding to Case 1

Starting Point / Sequent	P_{31} [0,-1000]		P_{32} [1000,-1000]		P_{33} [-1000,0]	
	Approach1	Approach2	Approach1	Approach2	Approach1	Approach2
1-3-2-1	3.5837	3.6361	4.138	3.7043	4.7971	5.2624
1-3-1-2	3.155	3.5679	3.7093	3.6361	4.3684	5.1942
1-1-3-2	3.0295	3.5679	3.5837	3.6361	4.2429	5.1942
1-1-2-3	2.3703	2.0098	2.9246	2.078	3.5837	3.6361
1-2-3-1	3.5837	3.6361	4.138	3.7043	4.7971	5.2624
1-2-1-3	2.4959	2.0098	3.0501	2.078	3.7093	3.6361
2-1-3-1	3.7093	3.6361	2.7855	3.7043	4.7971	5.2624
2-1-1-3	2.4959	2.0098	1.5721	2.078	3.5837	3.6361
2-3-1-1	3.5837	3.6361	2.66	3.7043	4.6716	5.2624
3-1-2-1	3.7093	3.6361	4.138	3.7043	2.8654	5.2624
3-1-1-2	3.155	3.5679	3.5837	3.6361	2.3111	5.1942
3-2-1-1	3.5837	3.6361	4.0124	3.7043	2.7398	5.2624

Table 3.6: Power required of UAV #3 corresponding to Case 1

(unit: $(m*kg/s)*10^{-5}$)

Starting Point / Sequent	P_{31} [0,-1000]		P_{32} [1000,-1000]		P_{33} [-1000,0]	
	Δ_{time}	Δ_{power}	Δ_{time}	Δ_{power}	Δ_{time}	Δ_{power}
1-3-2-1	0.48159	-0.0146	0.55407	0.1048	0.61765	-0.097
1-3-1-2	0.40704	-0.131	0.5	0.02	0.57857	-0.189
1-1-3-2	0.38097	-0.178	0.48159	-0.015	0.56557	-0.224
1-1-2-3	0.19519	0.1521	0.35736	0.2895	0.48159	-0.015
1-2-3-1	0.48159	-0.0146	0.55407	0.1048	0.61765	-0.097
1-2-1-3	0.23871	0.195	0.38541	0.3187	0.5	0.018
2-1-3-1	0.5	0.02	0.32314	-0.33	0.61765	-0.097
2-1-1-3	0.23871	0.19475	-0.26428	-0.32	0.48159	-0.015
2-3-1-1	0.48159	-0.015	0.28896	-0.393	0.60698	-0.13
3-1-2-1	0.5	0.02	0.55407	0.1048	0.34322	-0.84
3-1-1-2	0.40704	-0.13087	0.48159	-0.015	0.17289	-1.25
3-2-1-1	0.48159	-0.015	0.53949	0.077	0.31109	-0.921

Table 3.7: Comparative results for mission time and power required for UAV #3 corresponding to Case 1

Starting Point / Sequent	P_{21} [0,1000]		P_{22} [1000,1000]		P_{23} [1000,0]	
	Approach1	Approach2	Approach1	Approach2	Approach1	Approach2
1-3-2-1	2.682	2.7535	3.2363	2.7835	3.5259	3.141
1-3-1-2	3.1799	2.7235	3.7341	2.7535	4.0238	3.111
1-1-3-2	2.1277	2.7235	2.682	2.7535	2.9716	3.111
1-1-2-3	1.8381	2.366	2.3924	2.396	2.682	2.7535
1-2-3-1	2.682	2.7535	3.2363	2.7835	3.5259	3.141
1-2-1-3	2.8902	2.366	3.4445	2.396	3.7341	2.7535
2-1-3-1	3.7341	2.7535	2.8104	2.7835	3.5259	3.141
2-1-1-3	2.8902	2.366	1.9665	2.396	2.682	2.7535
2-3-1-1	2.682	2.7535	1.7582	2.7835	2.4738	3.141
3-1-2-1	3.7341	2.7535	3.2363	2.7835	2.5207	3.141
3-1-1-2	3.1799	2.7235	2.682	2.7535	1.9665	3.111
3-2-1-1	2.682	2.7535	2.1841	2.7835	1.4686	3.141

Table 3.8: Power required of UAV #2 corresponding to Case 2

(unit: $(m*kg/s)*10^{-5}$)

Starting Point / Sequent	P_{21} [0,1000]		P_{22} [1000,1000]		P_{23} [1000,0]	
	Δ_{time}	Δ_{power}	Δ_{time}	Δ_{power}	Δ_{time}	Δ_{power}
1-3-2-1	0.13935	-0.0267	0.2964	0.1399	0.35765	0.109
1-3-1-2	0.28309	0.14352	0.39548	0.26261	0.44126	0.223
1-1-3-2	-0.10794	-0.27999	0.13935	-0.026658	0.22925	-0.047
1-1-2-3	-0.30371	-0.28718	0.025707	-0.00151	0.13935	-0.0267
1-2-3-1	0.13935	-0.0267	0.2964	0.1399	0.35765	0.1092
1-2-1-3	0.20593	0.18139	0.34153	0.3044	0.39548	0.263
2-1-3-1	0.39548	0.26261	0.18165	0.0095599	0.35765	0.1092
2-1-1-3	0.20593	0.18139	-0.20904	-0.21842	0.13935	-0.0267
2-3-1-1	0.13935	-0.0267	-0.37047	-0.58312	0.06058	-0.2697
3-1-2-1	0.39548	0.26261	0.2964	0.1399	0.079569	-0.2461
3-1-1-2	0.28309	0.14352	0.13935	-0.026658	-0.20904	-0.5821
3-2-1-1	0.13935	-0.0267	-0.076475	-0.27442	-0.68308	-1.1388

Table 3.9: Comparative results for mission time and power required for UAV #2 corresponding to Case 2

Starting Point / Sequent	P_{11} [0,-1000]		P_{12} [1000,-1000]		P_{13} [-1000,0]	
	Approach1	Approach2	Approach1	Approach2	Approach1	Approach2
1-3-2-1	3.6086	3.3224	4.1628	3.3524	4.822	4.6484
1-3-1-2	3.1799	3.2924	3.7341	3.3224	4.3933	4.6184
1-1-3-2	3.0543	3.2924	3.6086	3.3224	4.2677	4.6184
1-1-2-3	2.3952	1.9965	2.9494	2.0265	3.6086	3.3224
1-2-3-1	3.6086	3.3224	4.1628	3.3524	4.822	4.6484
1-2-1-3	2.5207	1.9965	3.075	2.0265	3.7341	3.3224
2-1-3-1	3.7341	3.3224	2.8104	3.3524	4.822	4.6484
2-1-1-3	2.5207	1.9965	1.597	2.0265	3.6086	3.3224
2-3-1-1	3.6086	3.3224	2.6848	3.3524	4.6964	4.6484
3-1-2-1	3.7341	3.3224	4.1628	3.3524	2.8902	4.6484
3-1-1-2	3.1799	3.2924	3.6086	3.3224	2.336	4.6184
3-2-1-1	3.6086	3.3224	4.0373	3.3524	2.7647	4.6484

Table 3.10: Power required of UAV #3 corresponding to Case 2

(unit: $(m * kg/s) * 10^{-5}$)

Starting Point / Sequent	P_{11} [0,-1000]		P_{12} [1000,-1000]		P_{13} [-1000,0]	
	Δ_{time}	Δ_{power}	Δ_{time}	Δ_{power}	Δ_{time}	Δ_{power}
1-3-2-1	0.48159	0.079294	0.55407	0.1947	0.61765	0.036
1-3-1-2	0.40704	-0.0354	0.5	0.1103	0.57857	-0.0512
1-1-3-2	0.38097	-0.077961	0.48159	0.0793	0.56557	-0.0823
1-1-2-3	0.19519	0.16646	0.35736	0.31293	0.48159	0.0793
1-2-3-1	0.48159	0.079294	0.55407	0.19467	0.61765	0.036
1-2-1-3	0.23871	0.20798	0.38541	0.34098	0.5	0.1103
2-1-3-1	0.5	0.11025	0.32314	-0.193	0.61765	0.036
2-1-1-3	0.23871	0.20798	-0.26428	-0.269	0.48159	0.0793
2-3-1-1	0.48159	0.079294	0.28896	-0.249	0.60698	0.0102
3-1-2-1	0.5	0.11025	0.55407	0.195	0.34322	-0.608
3-1-1-2	0.40704	-0.0354	0.48159	0.079	0.17289	-0.977
3-2-1-1	0.48159	0.079294	0.53949	0.170	0.31109	-0.681

Table 3.11: Comparative results for mission time and power required for UAV #3 corresponding to Case 2

It is worth noting that Approach 2 may not reduce the mission time in certain scenarios. This can be seen from the results in Tables 3.5, 3.7, 3.9 and 3.11. For example, it is shown in Table 3.5 that Δ_{time} corresponding to scenario $S = (3,3,2,1,1)$ for UAV #2 is -1.424. This means that UAV #2 requires to fly from the location of formation F_3 to that of formation F_3 repeatedly, which represents a pathological scenario. This is, in fact, not a formation switching because it is not changing from one formation to another. Approach 2 may not save time in pathological scenarios.

The results obtained for formation switching can be summarized as follows.

1. Approach 2 reduce average mission time over all possible scenarios.
2. Approach 2 may lead to a higher average power required in formation switching, up to a maximum of 20% compared to Approach 1.
3. Approach 2 may not save time for pathologic scenario which requires reconfiguration to the same formation repeatedly.

3.3 Effect of Nonzero Acceleration

So far it is shown that the proposed approach can reduce the average reconfiguration time significantly. However, the required assumptions for this approach may not hold in some practical cases. For instance, the constant velocity assumption for the UAVs during the

reconfiguration period is not necessary valid in many applications. Hence, the impact of the acceleration component on the outcome of the proposed algorithm will be investigated next.

3.3.1 Formation Reconfiguration with Acceleration

The relationship between the displacement $\vec{d}$ and acceleration $\vec{a} = \dot{\vec{V}}(t)$ and the mission time is given by:

$$\vec{d} = \int_0^t \int_0^t \vec{a} dt \tag{3.26}$$

$$T_i = f(\vec{d}_i, \vec{V}_{max}, \vec{V}_l, \vec{a}) \tag{3.27}$$

where d_i denotes the overall displacement of the ith UAV. Assume that acceleration is nonzero, but constant in the leader frame. This is a realistic assumption in most applications. Consider two formation locations P_1 and P_2 in the leader frame and denote the distance $\overline{P_1P_2}$ between them with $|\vec{d}_L|$. The maximum velocity of each UAV in the leader frame is equal to $\vec{V}_{Lmax}$ and the relative acceleration $\vec{a}_L$ in this frame is assumed to be constant. The mission time in the absence of the acceleration will be:

$$T = \frac{|\vec{d}_L|}{|\vec{V}_{Lmax}|} \tag{3.28}$$

The mission time in the presence of constant acceleration, on the other hand, consists of three phases: acceleration phase whose duration is denoted by T_1, constant velocity phase with the duration ΔT, and deceleration phase whose duration is denoted by T_2. In the beginning of the mission, the velocities of the UAVs are equal and constant. In other words, the

velocity of each UAV in the leader frame is zero. Upon the issuance of the reconfiguration command, each UAV moves to its desired location in the new configuration in three steps.

1. Suppose the distance $|\vec{d}_L|$ is sufficiently long, i.e., $|\vec{d}_L| \geqslant \frac{|\vec{V}_{Lmax}^2|}{|\vec{a}_L|}$. The time durations T_1, T_2, and ΔT can then be expressed as (see Figure 3.12):

$$T_1 = T_2 = \frac{|\vec{V}_{Lmax}|}{|\vec{a}_L|} \tag{3.29}$$

$$\Delta T = \frac{|\vec{d}_L| - |\vec{a}_L| T_1^2}{|\vec{V}_{Lmax}|} \tag{3.30}$$

Note that ΔT is zero for the case when $|\vec{d}_L| = \frac{|\vec{V}_{Lmax}^2|}{|\vec{a}_L|}$, as shown in Figure 3.13.

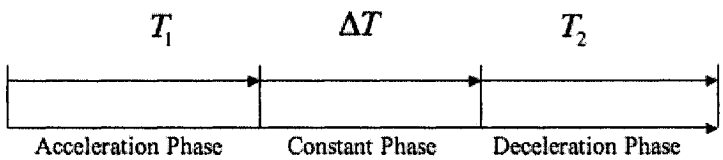

Figure 3.12: Three-phase reconfiguration for the case when $|\vec{d}_L| > \frac{|\vec{V}_{Lmax}^2|}{|\vec{a}_L|}$

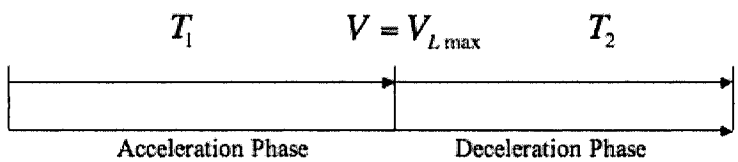

Figure 3.13: Three-phase reconfiguration for the case when $|\vec{d}_L| = \frac{|\vec{V}_{Lmax}^2|}{|\vec{a}_L|}$

Hence, the difference between the mission time with constant acceleration and with

zero acceleration in the leader frame can be presented as follows:

$$\begin{aligned} 2T_1 + \Delta T - T &= 2T_1 + \frac{|\vec{d}_L| - |\vec{a}_L|{T_1}^2}{|\vec{V}_{Lmax}|} - T \\ &= 2T_1 - \frac{|\vec{a}_L|{T_1}^2}{|\vec{V}_{Lmax}|} \\ &= T_1 \end{aligned} \tag{3.31}$$

2. Suppose that $|\vec{d}_L| < \frac{|\vec{V}_{Lmax}^2|}{|\vec{a}_L|}$. Then the time durations T_1 and T_2 can be expressed as (see Figure 3.14):

$$T_1 = T_2 = \sqrt{\frac{|\vec{d}_L|}{|\vec{a}_L|}} \tag{3.32}$$

It is to be noted that in this case $\Delta T = 0$. Therefore, $|\vec{d}_L| < \frac{|\vec{V}_{Lmax}^2|}{|\vec{a}_L|}$, and the difference

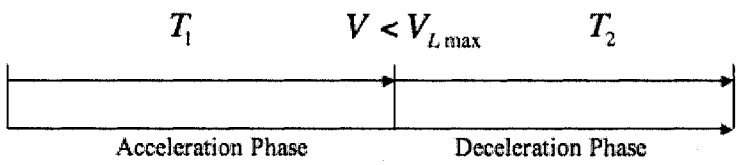

Figure 3.14: Three-phase reconfiguration for the case when $|\vec{d}_L| < \frac{|\vec{V}_{Lmax}^2|}{|\vec{a}_L|}$

between the mission time with constant acceleration and with zero acceleration in the leader frame in this case is given by:

$$\begin{aligned} 2T_1 + \Delta T - T &= 2T_1 + 0 - T \\ &= 2T_1 - \frac{|\vec{d}_L|}{|\vec{V}_{Lmax}|} \\ &= 2\sqrt{\frac{|\vec{d}_L|}{|\vec{a}_L|}} - \frac{|\vec{d}_L|}{|\vec{V}_{Lmax}|} \end{aligned} \tag{3.33}$$

An example will be presented now to clarify the above analysis. Consider the problem given in Example 3, and assume that the acceleration measured in the leader frame

is $|\vec{a}_L| = 3m/s^2$. The results obtained are given in Table 3.12. As it can be seen from this table, Δ_{time} corresponding to UAV #2 and #3 change from 44.9% to 43.81% and from 41.4% to 39.4%, respectively. These changes are very small, and are due to the fact that the dominators of the corresponding ratios in equation (3.20) increase, while the numerators remain unchanged. Hence, the resultant Δ_{time}'s for both UAVs are smaller compared to the zero-acceleration case. These results show that although the proposed algorithm is developed for the zero-acceleration case, it also reduces the reconfiguration time for a simple practical set-up with nonzero acceleration.

UAV #2				UAV #3			
Acceleration	Approach1	Approach2	Δ_{time}	Acceleration	Approach1	Approach2	Δ_{time}
Yes	378.95	212.95	43.81%	Yes	311.05	188.64	39.35%
No	325.72	194.22	44.9%	No	285.88	167.57	41.4%

Table 3.12: Reconfiguration time with and without acceleration

Chapter 4

Conclusions

4.1 Conclusions

A novel formation flying strategy is introduced in this work to minimize the reconfiguration time in UAV formation flying. It is assumed that a finite set of potential positions for each UAV in the formation is available. The reconfiguration is carried out in two stages. In the first stage, each UAV flies to a designated position which has the minimum average distance from all potential locations that it may fly to upon the issuance of the next reconfiguration command. In the second stage, the UAV flies from its designated position to the location assigned by the next reconfiguration command. The designated position is indeed a bridge between the two consecutive formations, and distinguishes the proposed method from the

traditional reconfiguration strategy, where each UAV stays at its present position upon the completion of a reconfiguration mission.

Throughout this work, it is assumed that there is a sufficiently long time gap between the two consecutive reconfiguration commands so that the proposed two-stage strategy can be carried out efficiently. Furthermore, the proposed method minimizes the average distance that each UAV requires to move during the entire mission, not the time. However, it is assumed that the velocity of each UAV is constant, and thus the distance it travels is proportional to the time. However, in order to save fuel, it may be desirable to fly with a lower speed during the idle time. Sufficient conditions are given which guarantee that the proposed method outperforms the traditional reconfiguration strategy. Simulation results show that even in the case of nonzero acceleration, the proposed method can reduce the reconfiguration time. It is to be noted that the assumptions made throughout the paper are generally realistic in practice, and has also been considered in several other relevant papers.

The simulation results presented in the thesis demonstrate the effectiveness of the proposed strategy in reducing the reconfiguration time for various formation scenarios. Furthermore, in many scenarios the proposed method also reduces the fuel consumption. It is shown that while the average time of reconfiguration is minimized, there are some pathological cases for which the traditional reconfiguration strategy would lead to a shorter mission time. The results of this research can have a significant impact on the time sensitive formation flying missions.

4.2 Suggestions for the Future Work

The effectiveness of the method proposed in this thesis for reducing the reconfiguration time depends on some important assumptions. This includes, for example, the assumption that the velocity of each UAV is constant. This assumption, although realistic in many applications, was mainly for reducing the complexity of the problem formulation. A more comprehensive study is needed to investigate the more general case, when acceleration and deceleration of the UAVs are not constant. This will lead to a more complex analysis as the relationship between distance and time cannot be expressed in a simple closed form in this case.

Another important assumption was that the idle time is sufficiently long so that the UAVs have enough time to settle in their SD position before the issuance of the next reconfiguration command. The case when the idle-time is not sufficiently long also needs further investigation.

Furthermore, the main development of the paper was based on the existence of a known set of potential formations. It was assumed in the analysis that this set is finite. Relaxing this condition would be a good direction for future research. In other words, the case when the potential configurations belong to a compact set can be considered by modifying the analysis presented in the thesis. One can also incorporate a probabilistic analysis in the new problem statement and the corresponding formulation. The probability

assigned to the compact set in this case will be a proper probability density function over the whole set. It is to be noted that the results obtained in the present work can be considered as a special case of the one described above.

Finally, a rigorous collision avoidance analysis would be very important in practice, specially in the case of a formation with several UAVs. Such analysis and how it changes the results obtained in this work can be another subject for future research.

Bibliography

[1] D. P. Scharf, F. Y. Hadaegh, and S. R. Ploen, "A survey of spacecraft formation flying guidance and control (part i): Guidance," *in Proc. of American Control Conference*, June, 2003.

[2] D. P. Scharf, F. Y. Hadaegh, and S. R. Ploen, "A survey of spacecraft formation flying guidance and control (part ii): Control," *in Proc. of American Control Conference*, June, 2004.

[3] R. K. Mehra, J. D. Boskovic, and S. M. Li, "Autonomous formation flying of multiple ucavs under communication failure," *Position Locations and Navigation Symposium, IEEE, New York*, 2000.

[4] D. W. Casbeer, D. B. Kingston, R. W. Beard, T. W. McLain, S. M. Li, and R. Mehra, "Cooperative forest fire surveillance using a team of small unmanned air vehicles," *International Journal of Systems Science, vol. 37, No. 6*, May, 2006.

[5] S. A. Cambone, K. J. Krieg, P. Pace, and L. Wells, "Unmanned aircraft systems (UAS) roadmap, 2005-2030," *Office of the Secretary of Defense*, 2005.

[6] D. S. Board, "Unmanned aerail vehicles and uninhabited combat aerial vehicles," *Defence Science Board For Acquisition, Technology and Logsitics, Washington, D.C. 20301-3140*, 2004.

[7] E. Bone and C. Bolkcom, "Unmanned aerial vehicles: Background and issues for congress," *Congressional Research Service/The Library of Congress*, April, 2003.

[8] J. Lavaei, A. Momeni, and A. G. Aghdam, "High-performance decentralized control for formation flying with leader-follower structure," *in Proc. of 45th IEEE Conference on Decision and Control*, to appear.

[9] J. R. T. Lawton, R. W. Beard, and B. J. Young, "A decentralized approach to formation maneuvers," *IEEE Trans. on Robotics and Automation, vol. 19, No. 6*, Dec, 2003.

[10] J. Desai, J. Ostrowski, and V. Kumar, "Controlling formations of multiple mobile robots," *IEEE Int. Conference, Robotics and Automation*, 1998.

[11] A. Pant, P. Seiler, and K. Hedrickr, "Mesh stability of look-ahead interconnected systems," *IEEE Trans. Automatic Control, vol. 47(2)*, 2002.

[12] M. Tillerson, L. Breger, and J. How, "Distributed coordination and control of formation flying spacecraft," *in Proc. of American Control Conference*, June, 2003.

[13] R. Beard and F. Hadaegh, "Constellation templates: An approach to autonomous formation flying," *World Automation Congress*, 1998.

[14] P. Wang, "Navigation strategies for multiple autonomous mobile robots moving in formation," *J. Robotic System, vol. 8(2)*, 1991.

[15] M. Anderson and A. Robbin, "Formation flight as a cooperative games," *AIAA Guidance, Nav., & Control Conference*, 1998.

[16] G. Campa, M. R. Napolitano, B. Seanor, and M. G. Perhinschi, "Design of control laws for maneuvered formation flight," *in Proc. of American Control Conference*, June, 2004.

[17] E. King, Y. Kuwata, M. Alighanbari, L. Bertuccelli, and J. How, "Coordination and control experiments on a multi-vehicle testbed," *in Proc. of American Control Conference*, June, 2004.

[18] Y. X. Hao, A. Davari, and A. Manesh, "Differential flatness-based trajectory planning for multiple unmanned aerial vehicles using mixed-interger linear programming," *in Proc. of American Control Conference*, June, 2005.

[19] I. Kaminer, O. Yakimenko, A. Pascoal, and R. Ghabcheloo, "Path generation, path following and coordinated control for time-critical missions of multiple UAVs," *in Proc. of American Control Conference*, June, 2006.

[20] D. P. Scharf, A. B. Acikmese, S. R. Ploen, and F. Y. Hadaegh, "A direct solution for fuel-optimal reactive collision avoidance of collaborating spacecraft," *in Proc. of American Control Conference*, June, 2006.

[21] M. Shanmugavel, A. Tsourdos, R. B. Zbikowski, B. A. White, C. A. Rabbath, and N. Lechevin, "A solution to simultaneous arrival of multiple UAVs using pythagorean hodograph curves," *in Proc. of American Control Conference*, June, 2006.

[22] D. R. Nelson, D. B. Barber, T. W. McLain, and R. W. Beard, "Vector field path following for small unmanned air vehicles," *in Proc. of American Control Conference*, June, 2006.

[23] R. S. Smith and F. Y. Hadaegh, "A distributed parallel estimation architecture for cooperative vehicle formation control," *in Proc. of American Control Conference*, June, 2006.

[24] C. Sultan, S. Seereeram, R. K. Mehra, and F. Y. Hadaegh, "Energy optimal reconfiguration for large scale formation flying," *in Proc. of American Control Conference*, June, 2004.

[25] W. Ren and R. W. Beard, "CLF-based tracking control for UAV kinematic models with saturation constraints," *in Proc. of* 42^{nd} *IEEE Conference on Decision and Control*, December, 2003.

[26] E. W.Frew, "Receding horizon control using random search for UAV navigation with passive, non-cooperative sensing," *No.80309, University of Colorado at Boulder, Colorado,*, 2005.

[27] J. J.Enright and E. Frazzoli, "UAV routing in a stochastic,time-varying environment," *No.90095, Mechanical and Aerospace Engineering, University of California Los Angeles Los Angeles CA*, 2005.

[28] A.W.Proud, M.Pachter, and J.J.D'Azzo, "Close formation flight control," *in Proc. of the AIAA Guidance, Navigation and Control Conference and Exhibit Portland, OR,*, 1999.

[29] W. Kang, A. Sparks, and S. Banda, "Coordinated control of multisatellite systems," *J. Guid., Control, and Dyn., vol. 24(2)*, 2001.

[30] H. Schuab, S. Vadali, J. Junkins, and K. Alfriend, "Spacecraft formation flying using mean orbital elements," *Astro. Sci., vol. 48(1)*, 1999.

[31] J. Hedrick, M. Tomizuka, and P. Varaiyar, "Control issues in automated highway systems," *IEEE Control System Magazine, vol. 14(6)*, 1994.

[32] J. Desai, J. Ostrowski, and V. Kumar, "Modeling and control of formations of nonholonomic mobile robots," *IEEE Trans. Robotics and Automation, vol. 17(6)*, 2001.

[33] M. E. Khatir and E. J. Davison, "Bounded stability and eventual string stability of a large platoon of vehicles using non-identical controllerss," *in Proc. of Conference on Decision and Control,*, December, 2004.

[34] X. H. Wang and S. Balakrishnan, "Optimal and hierarchical formation control for UAV," *in Proc. of American Control Conference*, June, 2005.

[35] E. Semsar and K. Khorasani, "Adaptive formation control of UAVs in the presence of unknown vortex forces and leader commands," *in Proc. of American Control Conference*, June, 2006.

[36] L. Dalla, "A note on the fermat-torricelli point of a d-simplex," *Journal of Geometry, vol. 70*, 2001.

[37] Q. Zuo and B. Lin, "Fermat points of finite point sets in metric spaces," *Journal of Math. (PRC) vol. 17*, 1997.

[38] N. D. Kazafinoff, "Geometric inequalities," *New York: Random House*, 1961.

[39] C. Kimberling, "Triangle centers and central triangles," *Congr. Numer. 129*, 1998.

[40] K. Schlude, "Distributed data & resources: Models, tractability, and complexity," *PhD thesis, Swiss Federal Institue of Technology Zurich*, 2002.

[41] T. W. McLain and R. W. Beard, "Unmanned air vehicle testbed for cooperative control experiments," *in Proc. of American Control Conference*, June, 2004.

[42] W. F. Phillips, "Mechanics of flight," *Hoboken, N.J. : Wiley*, 2004.

[43] C. D. Perkins, "Airplane performance stability and control," *New York, Wiley*, 1949.

Chapter 5

Appendix

5.1 Appendix A

5.1.1 Power required of UAVs

The power requirement of airplane is defined as energy per time [42], [43]. In Chapter 3, the expression for power requirement was given by equation (3.21), for the case when the UAVs fly at the same level and without accelerating. For a steady-level flight, the power required can be simplified as:

$$P_R = \frac{E}{t} = T_R V = DV \tag{5.1}$$

where V is the velocity of the aircraft, D is the draft of the UAV, and T_R is the thrust. To keep the flight at a steady level, the UAV needs a lift equal to its weight, i.e., $L = W$. Thus, one can obtain the following equation:

$$L = W = 1/2 C_L \rho V^2 S_w \tag{5.2}$$

where C_L is the coefficient of the lift. On the other hand, the thrust required for small angles is given by:

$$T_R = \frac{C_D}{C_L} W = (\frac{C_{D0}}{C_L} + C_{D0,L} + \frac{C_L}{\pi \ell R_A}) W \tag{5.3}$$

where R_A is the aspect ratio that $R_A := \frac{b^2}{S}$ and ℓ is a span efficiency factor, which ranges from 0.85 to 0.95 for typical subsonic aircraft. Combining the equations (5.2) and (5.3), the equation (5.1) can be rewritten as:

$$P_R = \left[\frac{C_{D0} \rho V^3}{2(W/S_w)} + C_{D0,L} V + \frac{2(W/S_w)}{\pi \ell R_A \rho V} \right] W \tag{5.4}$$

This is, in fact, the equation (3.21) used in Chapter 3. Typically, $C_{D0,L}$ in the above equation is equal to zero. The minimum power can be obtained by differentiating the above equation with respect to C_L, and setting the result to be equal to zero as follows:

$$\frac{\partial P_R}{\partial C_L} = \sqrt{2} \left[-\frac{3}{2} \frac{C_{D0}}{{C_L}^{5/2}} + \frac{1}{2} \frac{C_{D0,L}}{{C_L}^{3/2}} + \frac{1}{2} \frac{1}{\pi \ell R_A {C_L}^{1/2}} \right] W \sqrt{\frac{W/S_w}{\rho}} = 0 \tag{5.5}$$

which leads to the following results:

$$P_{Rmin} \cong \frac{4\sqrt{2} {C_{D0}}^{1/4}}{3\pi \ell {R_A}^{3/4}} W \sqrt{\frac{W/S_w}{\rho}} \tag{5.6}$$

$$C_L = \frac{\pi \ell R_A}{2} \left[C_{D0,L} + \sqrt{{C_{D0,L}}^2 + \frac{12 C_{D0}}{\pi \ell R_A}} \right] \tag{5.7}$$

5.1.2 Number of All Possible Formation Scenarios

Equation (3.23) in Chapter 3 was introduced to calculate the number of all possible scenarios of formation flying for a given number of UAVs. The equation is rewritten here:

$$N_s = M_s * \frac{L!}{\prod_{l=1}^{k} Q_l!} \tag{5.8}$$

This equation is obtained from the permutation and combination of all possible path planning for UAV formation flying. Define the set H as a set consisting of all formations, and call it the basic set for the formation. Then, L is the size of the basic set H. M_s is the number of all possible initial formations, which is the number of formations, indeed. The parameter k is the number of the subsets consisting of the repeated formations in the basic set H. For example, assume that there are three formations for a group of three UAVs. Assume also that the UAVs will fly to the formation F_1 twice as frequently as the other formations. Hence, the basic set H is $(1,1,2,3)$, L is equal to 4, and M_s is equal to 3. In this case, there is one subset of the repeated formations, i.e., (1,1), and hence, that $k = 1$.

Q_l is the size of the subset $l, l \in \bar{\mathrm{K}} := \{1,\ldots,k\}$. For example, in the basic set $H = (1,1,2,3)$, the subset of repeated formations will be the subset $(1,1)$. In this case, $k = 1$ and Q_1 will be the size of $(1,1)$ which is equal to 2.

It is required first to obtain the combination of all possible formation flying paths which is equal to $L!$. It is to be noted that if k is not zero, the repeated results should be taken into account. In other words, $L!$ needs to be divided by the number of repetitions, which is

$\prod_{l=1}^{k} Q_l!$. Finally, after adding the start locations, the number of all possible scenarios will be given by the equation (5.8).

For example, for the case when there are three formations for three UAVs with no repeated formation in the mission, $L = 3$, $M_s = 3$, and $k = 0$. One can easily verify that in this case $N_s = 3 * 3! = 18$.